Cell polarity and morphogenesis: Functions and mechanisms of cell divisions in vertebrate gastrulation

Thesis by

Ying Gong

In Partial Fulfillment of the Requirements

for the Degree of

Doctor of Philosophy

California Institute of Technology

Pasadena, California

2004

(Defended May 28, 2004)

Acknowledgements

Despite all the jokes graduate students like to tell about advisors, Dr. Scott Fraser, my advisor, has been a positive shaping force during my tenure in graduate school. Scott has given me the freedom and support to develop and pursue my research interest. And through his uniquely sarcastic yet good humored way, he has offered insightful criticism when criticism is due.

I am grateful to members of my thesis committee, Dr. Marianne Bronner-Fraser, Dr. Paul Sternberg, and Dr. Kai Zinn for their encouragement and guidance.

Many past and present members of the Fraser lab have made it pleasant to wake up in the morning to go to the dungeony lab (it is in the basement with no windows). They are not only my colleagues, but my mentors and friends. In particular, Dr. Reinhard Köster taught me all the zebrafish techniques to get started and helped me tremendously with molecular biology. Dr. David Koos, with his solid knowledge base in early patterning of zebrafish, has endured my frequent sessions of brain-picking. Dr. Helen McBride has helped me hone my presentation skills and is a walking encyclopedia of molecular biology. Mary Flowers, our lab mom has kept the lab in check and made ordering reagents ridiculously easy for us. Aura Keeter has offered excellent technique assistance. Dr. John Wallingford at UT Austin, an unofficial member of the lab, has been a great resource for my project and was the gatekeeper for my manuscript.

My other friends at Caltech have enriched various aspects of my life. I have especially benefited from my good friend Chunhui Mo's encouragement and out-of-the-box ideas.

Finally, I would like to thank my parents and my sister. My parents have endured great hardships in life but have never faltered in giving unconditional love and support to their daughters. My sister, also my closest friend, gives me the courage to take risks and venture into the unknown. Because I know no matter what happens, she will be there for me.

With all of its up and downs, my six years at Caltech is, I summarize, a fun time.

Abstract

Gastrulation shapes a vertebrate embryo from an egg-shaped aggregate of cells. In many vertebrates, massive cell divisions occur during gastrulation. In this thesis, I investigate the pattern, function, and regulation of mitotic divisions in zebrafish gastrulation. Using in vivo confocal imaging and quantitative analysis, I find that cells in dorsal axial tissues preferentially divide along the direction of tissue elongation, i.e., the anterior-posterior axis of the embryo. Establishment of the spindle polarity requires Silberblick/Wnt11, Dishevelled and Strabismus acting via the non-canonical Wnt/planar cell polarity (Wnt/PCP) pathway. On the subcellular level, oriented cell division is mediated by spindle rotation. The mitotic spindle forms at a random orientation and rotates at metaphase to line up with the anterior-posterior axis. Wnt/PCP signalling is not required for the spindle to rotate but dictates its destination. These data, together with previous work by others, demonstrate that cell polarization underlies the morphogenetic machinery that shapes the head-to-tail axis. In addition, Wnt/PCP signalling is involved in polarizing the cells, whose responses include medial-lateral elongation of the cell body and localization of protrusions, and anterior-posterior positioning of the mitotic spindle. These two types of polarized cell behaviours cooperate to shape the anterior-posterior body axis of the embryo. This work also demonstrates that the Wnt/PCP pathway is evolutionarily conserved as a strategy for cell polarization.

Table of Contents

List of Figures

Chapter 1

Introduction: cell polarity and formation of the head-to-tail axis

Goal of thesis

The goal of my thesis was to study morphogenesis, the processes that shape the body of an animal. I focus on the early development of the embryo because this is the time when the most critical events take place. Development is in essence a process of pattern formation. The basic pattern, or body plan, emerges at the earliest stages of embryogenesis, and later development continuously refines and elaborates this basic body plan. Pattern formation has two components: differentiation, the process by which one group of cells become different from others, and morphogenesis, the process by which cells create forms. I chose to study the latter because we knew less about it mechanistically. Since the coming together of genetics and development, a lopsided majority of research has focused on differentiation, a problem that can be explained and described in terms of differential gene expression from the same genome present in every cell. A large amount of knowledge has been accumulated on signal transduction and transcriptional controls (and to a lesser extent post-transcriptional controls) that lead to differential gene expression. By comparison, the study of morphogenesis, to a large extent, has stayed within the realm of classical embryology. However, creation of body form is also a result of regulated expression of genes—those encoding the mechanical properties of cells. Signals involved in differentiation can also regulate morphogenesis but their targets are proteins that regulate the cytoskeleton, cell adhesion, extracellular matrix and other mechanical properties rather than those proteins that determine cell fate. As such, the problem of morphogenesis, which is a

biomechanical problem, can be addressed using tools and concepts of modern developmental biology and cell biology.

On a more practical level, I chose to focus on morphogenesis because I felt that the resources available in the Fraser lab could allow me to take an integrated approach in my research. By applying the concepts and methods of molecular biology, cell biology, and embryology, I could start to understand how gene activities lead to the subcellular and cellular behaviors that effect the macroscopic changes in embryo shape.

Research framework

The specific subject matter for my thesis is cell division polarity during gastrulation. A large number of cell divisions occur during vertebrate gastrulation, a period when striking changes of body shape occur. The aim of this thesis work is thus to understand the functional significance of these cell divisions in the context of morphogenesis and the controlling mechanisms. Towards this end, I employed a three-tiered approach. I first characterized the pattern of cell divisions during normal morphogenesis. Then, I perturbed the functions of several candidate genes and examined the effects on the division patterns and morphogenesis. Finally, I began to probe the subcellular machinery through which genes exerts controls on division patterns. Because cell division patterns are not binary, a prerequisite for using this framework is the ability to quantitatively characterize cell divisions. This involved a great deal of painstaking

manual tracking and highlighted the need to develop computer algorithms to extract large amounts of quantitative data.

Choice of experimental system

I chose to use the zebrafish *Danio rerio* for my study for several reasons. The zebrafish embryo is easily accessible for a variety of embryological manipulations since it develops outside the mother in a Petri dish and develops normally at a rather wide range of temperatures from 20 to 30^{o}C. The transparency of the zebrafish embryo, an attribute unparalleled by other vertebrate model organisms including frog, chick and mouse, make it well suited for imaging studies of morphogenetic processes. The zebrafish genes are also amenable to study. When I started the project, the large-scale mutagenesis screen of developmental genes had finished, yielding over 1000 mutants with defects in more than 300 genes (Haffter et al., 1996). Among these mutants are a handful that have defects in early morphogenesis (Hammerschmidt et al., 1996). Other gene manipulation techniques, including RNA overexpression and morpholino knock-downs also work robustly in zebrafish.

Shaping the vertebrate body

The vertebrate body plan emerges at gastrulation when a set of coordinated morphogenetic processes transform the egg-shaped embryo into a

"miniature adult." One of the most prominent accomplishments of gastrulation is that the anterior-posterior body axis is extended, with the head on one end of the axis and the tail on the other. Most studies of axis elongation in the last decade focus on the patterns and regulations of polarized cell movements in the amphibian *Xenopus laevis* and more recently also in the zebrafish. Therefore, the first few subsections will be dedicated to reviewing the large amount of literature concerning these cell movements. I will then discuss what is known about cell division in the context of axis elongation.

Tissues forming the anterior-posterior axis

The anterior-posterior axis of an embryo is the line that connects the head and tail. The tissues lining the anterior-posterior axis, known as the axial tissues, include the notochord, prechordal plate and the overlying neural tissue. The somitic mesoderm is lateral to the notochord and is called the paraxial tissue. During gastrulation, these axial and paraxial tissues collectively narrow and extend to form a long column that will become the backbone of the embryo. This end result of narrowing and lengthening is often referred to as convergence and extension, and is used interchangeably with the term "axis elongation" in this introduction. Convergence and extension are more prominent in the posterior tissues. The anterior neural plate and the prechordal plate extend moderately, and probably converge even less (see below).

Cell movements underlying *Xenopus* axis elongation

Keller and colleagues have studied axis elongation in the perspective notochord and somitic mesoderm, and the posterior neural ectoderm of *Xenopus* (Keller et al., 2000). Explants of these tissues extend autonomously by two types of cell rearrangement. In the first half of gastrulation, the cells intercalate along the radius of the embryo (radial intercalation) to produce a thinner and longer array (Keller et al., 1992; Wilson and Keller, 1991). In the second half of gastrulation and through much of neurulation, cells intercalate medial-laterally (medial-lateral intercalation) to form a narrower and longer array (Keller et al., 1992; Shih and Keller, 1992b). This mediolateral intercalation results in simultaneous convergence and extension of the tissue, and is often referred to as “convergent extension”.

The notochord and somitic mesoderm, and the posterior neural plate produce the most elongation. Other axial tissues also extend along the anterior-posterior orientation. The prechordal plate mesoderm migrates along the blastocoel roof towards the animal pole. During migration, cells also intercalate radially, resulting in tissue extension along the anterior-posterior axis (Davidson et al., 2002). The anterior neural plate, located in the animal region, thins by radial intercalation and expands in area during late blastulation and gastrulation. The increase in area may be uniform in all directions, unlike the radial intercalation of the marginal region (the prospective notochord, somitic mesoderm and posterior neural plate) (Keller, 1980).

Cell movements underlying zebrafish axis extension

The spatial and temporal patterns of cell movements underlying axis extension in zebrafish have not been examined as systematically as in *Xenopus*. Nonetheless, medial-lateral intercalation narrows the notochord and somitic mesoderm, and the overlying posterior neural plate (Glickman et al., 2003; Kimmel et al., 1994). Cells in the more lateral regions move toward the dorsal midline but do not undergo much intercalation before reaching the paraxial region (Myers et al., 2002).

Anterior migration also occurs in the prechordal plate in zebrafish (Ulrich et al., 2003). The prechordal plate elongates during gastrulation but how this happens is not known. Throughout gastrulation, the entire blastoderm undergoes epiboly to enclose the yolk (Warga and Kimmel, 1990). This motion also contributes to elongation of the anterior-posterior axis.

Cell polarization during *Xenopus* medial-lateral intercalation

Polarized movements must be accompanied by polarization of the cells carrying out the movements. Polarized cell behaviors have indeed been revealed by time-lapse studies of *Xenopus* explants undergoing medial-lateral intercalation (reviewed in (Keller, 2002; Keller et al., 2000; Wallingford et al., 2002). In the dorsal mesoderm explants, cells are round and transiently extend randomly oriented lamellipodial protrusions before they engage in intercalation. Then these cells become elongated along the medial-lateral axis, and more stable protrusions are localized to the medial and lateral ends of the cells (Shih

and Keller, 1992a). It is proposed that cells use these polarized protrusions to pull themselves between their medial-lateral neighbors (Keller et al., 2000).

In the posterior neural plate explants, cells are also polarized as they undergo intercalation. They become medial-laterally elongated as is the case for mesodermal cells (Elul and Keller, 2000; Elul et al., 1997; Ezin et al., 2003). However, neural cells can acquire different types of protrusive activities depending on interactions with the underlying mesoderm. In neural plate explants without the underlying mesoderm, no midline floor plate is formed. Cellular protrusions are bipolar, forming at both the medial and lateral ends (Elul et al., 1997). In neural plate explants with underlying mesoderm, a midline floor plate is formed. Cellular protrusions are monopolar, forming at the medial ends only (Elul and Keller, 2000).

Cell polarization in other cell movements during *Xenopus* axis elongation

As noted above, both the dorsal mesoderm and neural plate carry out radial intercalation in the early stages of gastrulation. It is technically difficult to observe cell behaviors, especially the small cellular protrusions, along the radial axis. A scanning electron microscopy study by Keller suggests that cells are polarized along the radial axis during radial intercalation (Keller, 1980).

Time-lapse recordings of prechordal plate explants reveal that polarized cell behaviors underlie anterior migration and radial intercalation (Davidson et al., 2002). Cells form monopolar protrusions directed at their movement direction.

Cell polarization during zebrafish axis elongation

The protrusive activity of cells engaging in medial-lateral intercalation is yet to be described in detail in the zebrafish, though certain similarities to the *Xenopus* system are expected. Cells in axial and paraxial tissues take a medial-lateral elongated shape during late gastrulation (Concha and Adams, 1998; Jessen et al., 2002; Marlow et al., 2002; Topczewski et al., 2001).

In the migrating prechordal plate, cells at the leading edge orient cellular protrusions along their individual movement directions (Ulrich et al., 2003).

Molecular controls of axis elongation and polarized cell movements

Identifying and understanding the molecular controls of morphogenesis requires a different conceptual framework from what is used in cell fate determination. Genes involved in cell fate determination generally fit the scheme of signaling—transcription factor—cell fate. On the other hand, genes regulating morphogenesis work in the scheme of signaling—polarity complex—cell motility. As cell fate and cell motility are both outcomes of pattern formation, upstream factors controlling pattern formation will of course influence both processes. But these factors are not directly regulating cell motility and are therefore not included in the discussion.

A number of genes that affect axis elongation without affecting cell fate have been identified in both *Xenopus* and zebrafish. Among these are genes that are homologs to the *Drosophila* planar cell polarity genes (Veeman et al., 2003a; Wallingford et al., 2002).

The planar cell polarity pathway

Epithelia are polarized along their apical-basal axis. Some epithelia are also polarized within the epithelial plane. This is known as planar cell polarity or PCP. The best studied examples of PCP are those of the *Drosophila* adult wing and eye. In the wing, each cell has a single hair that points distally. In the eye, each ommatidium has 8 photoreceptor cells that are arranged in an oriented pattern (Strutt, 2003).

PCP in both tissues are affected by a set of "core" PCP genes that include the putative Wnt receptor Frizzled (Fz), the transmebrane proteins Van-Gogh/Strabismus (Stbm), the seven-pass transmembrane cadherin Flamingo (fmi), and the intracellular proteins Dishevelled (Dsh) and Prickle (Pk) (Strutt, 2003; Tree et al., 2002). These core PCP proteins are asymmetrically localized within the cell, presumably in response to a polarizing signal. The polarity information is then relayed from the PCP complexes to downstream machineries that lead to the polarized morphology of the cell.

Fz and Dsh also function in the well-studied Wg signaling pathway that involves GSK-3, Axin, and β-catenin (Cadigan and Nusse, 1997). Therefore, the PCP pathway is known as the non-canonical Wnt pathway (though a Wnt ligand has not been implicated in *Drosophila* PCP), to distinguish from the canonical Wnt (Wg)/ β-catenin pathway.

The PCP pathway regulates axis elongation in both Xenopus and zebrafish

Evidence for a non-canonical Wnt pathway's involvement in morphogenesis first came from misexpression studies in *Xenopus* embryos. While the "canonical" Wnts induce a secondary axis when expressed ectopically on the ventral side, overexpression of XWnt5, XWnt4, or Xwnt11 does not induce a secondary axis but affects morphogenesis (Du et al., 1995; Moon et al., 1993). Different ability in secondary axis induction and morphogenesis was also observed with Frizzled receptors. Overexpression of XFz7 affects morphogenesis without inducing a secondary axis (Djiane et al., 2000). XFz7 and XWnt11 interact both biochemically and functionally. Furthermore, studies using Dsh domain deletions show a parallel of domain requirement between PCP and convergence and extension. (Axelrod et al., 1998; Heisenberg et al., 2000; Rothbacher et al., 2000; Tada and Smith, 2000; Wallingford et al., 2000).

In addition to these overexpression experiments with wild-type and mutant molecules, zebrafish loss-of-function mutants in *silberblick (slb)/wnt11* and *pipetail (ppt)l/wnt5* mutants both exhibit morphogenetic defects without fate transfromation (Heisenberg et al., 2000; Kilian et al., 2003; Rauch et al., 1997). *slb* is expressed in the anterior paraxial tissue while *ppt* in the posterior axial and paraxial tissue. Single mutants have weak axis extension phenotype with slb mutants showing extension defect in more anterior tissues and ppt mutants in the posterior body. *slb; ppt* double mutants have more severe defects suggesting these two genes collaborate in regulating convergence and extension of the axis (Kilian et al., 2003).

Additional evidence of a PCP-like pathway in regulating morphogenesis has come from analysis of vertebrate homologs of *Drosophila* genes that are specific to PCP (Strutt, 2003). These genes include *stbm* (Darken et al., 2002; Goto and Keller, 2002; Jessen et al., 2002; Park and Moon, 2002), *pk* (Carreira-Barbosa et al., 2003; Takeuchi et al., 2003; Veeman et al., 2003b), and *fmi* (Formstone, C. J., personal communication). RNA overexpression, loss-of-function mutation, and morpholino gene knockdown of each gene leads to similar defects in axis extension in zebrafish and *Xenopus*. The loop-tail mouse, which has a mutation in a *stbm* homolog, fails to close its neural tube, likely due to defective convergence of the neural plate (Kibar et al., 2001; Wallingford and Harland, 2002). Similar phenotype is observed in the Celsr1 mouse, which harbors a mutation in the homolog to the *fmi* gene (Curtin et al., 2003).

The PCP pathway mediates polarized cell behaviors in axis elongation

Drawing on PCP's role in regulating cell polarity in epithelia, PCP is likely to regulate polarized cell movements during axis elongation. Wallingford and colleagues proved this to be the case (Wallingford et al., 2000). In *Xenopus* dorsal mesoderm explants, cells expressing mutant Xdsh lose their medial-laterally elongated morphology and the biopolar protrusions become randomized. Similar disruption of cell polarity and medial-lateral intercalation by overexpression of *Stbm* mRNA is observed in both mesoderm and neural plate in *Xenopus* (Goto and Keller, 2002). In zebrafish, defects in medial-lateral polarity and polarized movements of axial and paraxial cells are also found in mutants

and morphants of the PCP genes (Jessen et al., 2002; Kilian et al., 2003; Veeman et al., 2003b).

Downstream mechanisms of PCP in regulating polarized cell movements

The PCP signal has to be relayed to cellular machineries that create the polarized cell behaviors. Since cells elongate and have polarized protrusions in response to PCP, the cytoskeleton is a likely target. Cytoskeletal rearrangement may require the small GTPases Rho and Rac, which are known regulators of the actin cytoskeleton (Etienne-Manneville and Hall, 2002). In *Xenopus*, Rho and Rac are activated in the dorsal axial tissues during gastrulation and this activation requires PCP signaling. A novel protein, Daam-1, associates with Rho and Dsh, and mediates Dsh-Rho complex formation in cultured human cells. Rac directly binds Dsh in the same type of assay. Disrupting Rho, Rac, or Daam-1 causes defects in convergence and extension (Habas et al., 2003; Habas et al., 2001). In zebrafish, a homolog of the Rho effector protein Rho-associated kinase (Rok2) has been shown to act downstream of the non-canonical Wnt pathway to regulate convergence and extension as well as cell polarization (Marlow et al., 2002).

Other molecules involved in regulating axis elongation

Fibronectin and integrin

In *Xenopus*, cell interaction with the extracellular fibronectin matrix, mediated by the α5β1 integrin receptor, is essential for many morphogenetic processes. These include the anterior migration of the prechordal plate (Davidson et al., 2002; Winklbauer and Keller, 1996; Winklbauer and Nagel, 1991), the radial and medial-lateral intercalation of the dorsal mesoderm (Marsden and DeSimone, 2001; Marsden and DeSimone, 2003), as well as the radial intercalation underlying epiboly of the animal region (Marsden and DeSimone, 2001). Disrupting the fibronectin-integrin interaction compromises the medial-lateral elongation of the cells, indicating polarization of cells is influenced by their interaction with the extracellular matrix (Marsden and DeSimone, 2003).

C-cadherin and axial and paraxial protocadherins are also implicated in convergence and extension (Kim et al., 1998; Lee and Gumbiner, 1995; Yamamoto et al., 1998; Zhong et al., 1999). Fibronectin-integrin interaction may modulate C-cadherin adhesion (Marsden and DeSimone, 2003). How these adhesion molecules work in polarized cell movements remains to be determined. They could either signal to influence cell polarity or affect mechanical interactions between already polarized cells with each other or the extracellular matrix.

Calcium

Gastrulation in zebrafish and *Xenopus* involves oscillations of calcium levels. Intercellular calcium waves have been observed using calcium sensitive

indicators and time-lapse images in whole zebrafish embryos and *Xenopus* dorsal mesoderm explants (Gilland et al., 1999; Wallingford et al., 2001).

Calcium waves may be involved in coordinating convergent extension. In *Xenopus*, calcium waves are observed in the dorsal but not the ventral mesoderm explants. Blocking calcium release using pharmacological agents leads to defects in convergent extension in *Xenopus* (Wallingford et al., 2001). However, the spatial pattern of calcium waves in whole zebrafish embryos during zebrafish gastrulation does not clearly indicate a role in convergence and extension. During the first half zebrafish gastrulation, calcium hot spots seem to be randomly distributed around the entire blastoderm margin. Calcium waves are initiated at one of these spots and propagate around the margin. After about 85% epiboly, the wave initiation zone becomes restricted to the dorsal margin, which becomes incorporated into the developing tail bud after gastrulation. Calcium waves continue to spread from the tail bud zone throughout the caudal half of the embryo. Some of these "tail bud pulses" continue up to the head, along either dorsal or ventral routes (Gilland et al., 1999).

How gastrulation calcium waves are regulated is not clear. Modulation of intracellular calcium level is the outcome of multiple signaling pathways such as the non-canonical Wnt pathway and FGF pathway and it is possible more than one pathway is involved in this scenario. Mechanisms regulating the intercellular propagation of calcium are even more elusive.

Other molecules

Other molecules are also implicated in regulating convergence and extension based on overexpression studies. These include Sprouty, an intracellular antagonist of FGF signaling and Slit, a gene identified for its role in axon guidance (Nutt et al., 2001; Yeo et al., 2001). How these genes regulate the cell behaviors underlying convergence and extension is unknown.

Cell division and axis elongation

Concha and Adams used Nomarski microscopy to study cell divisions in the superficial epiblast layer from blastula to neurula stages in zebrafish (Concha and Adams, 1998). Divisions in the blastula appear to be along randomly orientations. They can be planar—parallel to the surface of the embryo, radial—parallel to a radius, or oblique—at a angle intermediate to the two. When gastrulation begins, divisions in this superficial layer gradually become planar. Furthermore, they become aligned such that the daughter cells separate along the anterior-posterior axis. When neurulation begins, orientation of cell divisions gradually switches to align with the medial-lateral axis of the embryo (i.e., a 90^{o} change). One result of these medial-lateral divisions is the generation of bilateral sister cell pairs in the neural tissue (Concha and Adams, 1998; Kimmel et al., 1994; Papan and Campos-Ortega, 1994).

In addition to oriented cell division in zebrafish, anterior-posterior oriented division also happens during avian primitive streak extension (Wei and Mikawa, 2000), in notochord in avian (Sausedo and Schoenwolf, 1993) and mouse (Sausedo and Schoenwolf, 1994) and neural plate (Sausedo et al., 1997;

Schoenwolf and Alvarez, 1989). How these oriented cell divisions are regulated remains an open question. In Chapter 2 of this thesis, I investigated in detail the patterns of cell divisions in the zebrafish axial tissues during gastrulation. I then studied the molecular controls for these stereotyped patterns of cell divisions. In Chapter 3, I took the investigation to the subcellular level and examined behaviors of the mitotic spindle responsible for the division patterns.

Chapter 2

Planar cell polarity signaling controls orientation of cell divisions during zebrafish gastrulation

Ying Gong, Chunhui Mo & Scott E. Fraser

Part of this chapter is to appear in *Nature*

Abstract

Oriented cell division is an integral part of pattern development in processes ranging from asymmetric segregation of cell-fate determinants to the shaping of tissues (Ahringer, 2003; Sausedo et al., 1997). Despite the many proposals that it can play an important role in tissue elongation (Schoenwolf and Alvarez, 1989; Wei and Mikawa, 2000), the mechanisms regulating division orientation have been little studied outside of the invertebrates *Caenorhabditis elegans* and *Drosophila melanogaster* (Ahringer, 2003). Here, we have analyzed mitotic divisions during zebrafish gastrulation using in vivo confocal imaging and find that cells in dorsal tissues preferentially divide along the animal-vegetal axis of the embryo. Establishment of this animal-vegetal polarity requires the Wnt pathway components Silberblick/Wnt11, Dishevelled and Strabismus. Our findings demonstrate an important role for non-canonical Wnt signalling in oriented cell division during zebrafish gastrulation and indicate that oriented cell division is a driving force for axis elongation. Our results suggest that non-canonical Wnt signaling plays a conserved role in vertebrate axis elongation by orientating cell elongation axis and division axis.

Introduction

Gastrulation in zebrafish starts as the blastoderm begins to cover the yolk cell. Mesendoderm precursors internalize near the blastoderm margin to form an inner blastoderm stratum termed the hypoblast. Cells remaining in the outer stratum constitute the epiblast, which give rise to neural ectoderm on the dorsal side and epidermis on the ventral side (Kimmel et al., 1995). The dorsal epiblast consists of 2 to 3 layers of cells, most of which divide twice during gastrulation: once near the start of gastrulation and another in mid gastrulation (Kimmel et al., 1994; Woo and Fraser, 1995). Mitotic divisions at different stages appear random, oriented animal-vegetally (AV), or oriented mediolaterally (ML) (Concha and Adams, 1998; Kimmel et al., 1994). Neither the full extent nor the mechanisms that regulate division orientation have been explored. Thus, we have characterized the patterns of cell division throughout the depth of the dorsal epiblast during zebrafish gastrulation and have investigated its molecular control.

Methods

Fish

Maintenance of adult zebrafish (Danio rerio) was carried out according to the Zebrafish Book (Westerfield, 1995). silberblick/Wnt11 homozygous embryos were selected from clutches produced by heterozygous mating pairs (Heisenberg et al., 2000) and raised to adulthood.

mRNA and morpholino injection

Capped mRNA was injected into one-cell stage embryos. The following dosages were used: Xdd1 (also known as Xdsh-ΔPDZ) 500 pg, Xdsh-DEP+ 800 pg, Xdsh-D2-GFP 500 pg, Zdkk1 500 pg, B-galactosidase 500 pg (control). For cell division experiments, each mRNA was co-injected with 100 pg H2B-GFP (Koster and Fraser, 2001) or H2B-mRFP1 (Campbell et al., 2002) mRNA. For Xdd1 mosaic experiments, a single cell at the 16 to 32 cell stage was injected with approximately 40 pg Xdd1 and 10 pg H2B-GFP mRNA. For ICAT mosaic experiments, a single non-marginal cell at the 64 cell stage was injected with approximately 40 pg of the mouse ICAT mRNA and 10 pg H2B-GFP mRNA. For double labelling experiments, 200 pg membrane-mRFP1 was also injected. Morpholino for the zebrafish Strabismus mRNA was previously described (Park and Moon, 2002) . 2 ng of morpholino was co-injected with 100 pg H2B-GFP into one-cell stage embryos.

In vivo imaging

Embryonic shield stage embryos were dechorionated and mounted in 1.3% low gelling point agarose in a custom-made imaging chamber. Four-dimensional (4D) confocal time-lapse imaging was carried out on an upright Zeiss LSM 510 or an inverted LSM PASCAL laser scanning microscope. z-stacks were collected at 1.5 to 2 minute intervals and spacing between consecutive z slices was set to values recommended by the microscope controlling software (typically around 2 μm). Embryos were imaged for 3.5 to 4 hours to approximately bud stage. The 488 nm laser line was used for imaging GFP and 543nm for RFP. Low laser power was used to minimize phototoxicity. Development of each embryo was monitored after the imaging session and embryos showing abnormal necrosis were not included for analysis.

Analysis of cell division orientation

4D images were visualized using the Zeiss LSM software. Cell divisions (division 15, which occurs after the embryonic shield stage (Kimmel et al., 1994)) were easily identified in H2B-GFP labeled cells because of changes in chromatin arrangement during mitosis. For each mitotic division, x, y, z coordinates of the two daughter cell nuclei were recorded. Only nuclei within a 150 um square area centered at the dorsal midline and equator were used for analysis. The local curvature of the embryo within this region was minimal and thus not considered in our analysis. Each embryo was mounted such that the medial-lateral axis corresponds to the x axis, the animal-vegetal axis corresponds to the y axis, and the depth axis corresponds to the z axis of the images (Fig. 2b). A line was

drawn between the two daughter nuclei and the angle between this line and the AV axis was calculated. Since the angle is in 3D, we broke it down into two planar projections: one in the epiblast plane (α) and one in the plane perpendicular to it (β). 0^{o} represents divisions whose planar components are parallel to the AV axis while 90^{o} represents divisions whose planar components are orthogonal to the AV axis (Fig. 2b). All calculations were performed using custom routines written in MATLAB.

Analysis of cell elongation orientation

Cell shape was determined in interphase immediately before mitosis (approximately 12 minutes before anaphase). From each 3D stack, the frame across the centre of the nucleus was selected for analysis. LWRs and cell elongation angles were measured using the best-fit ellipse function in NIH image.

Results

Mitotic divisions are oriented along the animal-vegetal axis

To monitor mitotic divisions through the depth of the epiblast, we imaged zebrafish gastrulae ubiquitously expressing Histone 2B fused to green fluorescent protein (H2B-GFP) using four-dimensional (4D: x, y, z, t) confocal microscopy (Fig. 2a). H2B-GFP marks the chromatin and renders mitosis easily visible in time-lapse movies due to the changes in the shape of the chromosomes during mitosis. Different cell layers can also be easily distinguished by the size and relative movement of the nuclei (Fig. 1). The deep cells have small nuclei (Fig. 1b, c, d) and move more rapidly relative to the overlying enveloping layer (EVL) (data not shown). The epiblast (presumptive ectoderm) and hypoblast (presumptive mesendoderm) can be distinguished in time-lapse movies by the direction of their movements (not shown). In this paper, we focus on the epiblast. The hypoblast, which is deeper into the embryo, is not imaged clearly to allow accurate analysis.

Division orientation in the dorsal epiblast is determined from the 4D images by measuring the angle between the mitotic spindle and the AV axis (Fig. 3b). Each angle is characterized by its two planar projections: α, the angle within the epiblast plane; β, the angle within the perpendicular plane. Analysis in wild-type gastrulae showed that divisions in all layers of the dorsal epiblast are oriented along the AV axis (Fig.3a-d, i-l). Over 90% of α angles are under 45 ^{o};

58% are under 20° (Fig. 3q). Similarly, 95% of β angles are under 45°; 62% are under 20° (Fig. 3r).

Division orientation is not a result of the mechanical force generated by cell geometry

Previous observations have shown that the mitotic spindle tends to align with the cell's long axis due to geometric constraints (known as Hertwig's rule) (Black and Vincent, 1988; Hertwig, 1893). To investigate whether this is the case in our system, we examined the relationship between dorsal epiblast cells' division orientation and their morphology by double-labeling the cells with a membrane RFP and H2B-GFP. In our time-lapse movies, a majority (92%) of the dorsal epiblast cells in wild-type embryos elongate with a ML bias at interphase (Fig. 4a-d; green circles in Fig. 4i; length to width ratio, or LWR = 1.66 ±0.45). During mitotic division, these cells round up and divide to create daughter cell pairs that separate in the AV orientation (Fig. 4a-d, j). Perhaps not surprisingly given this, in 65% of the cases, the angle between a cell's long axis during interphase and its spindle during mitosis is within 10° of perpendicular (Fig. 4k). Thus most cells divide nearly orthogonal to their long axis, the opposite of the expectation from Hertwig's rule.

AV orientation of cell division requires Dishevelled signaling

The above findings suggest that the mitotic spindle is actively oriented in the dorsal epiblast, and prompted us to investigate the molecular mechanisms underlying this process. Signaling through Dishevelled (Dsh) has been

implicated in polarized division in *Drosophila* and *C. elegans* (Ahringer, 2003; Bardin et al., 2004), raising the possibility that it regulates oriented division in the zebrafish gastrulae.

To assess the function of Dsh, we injected into zebrafish embryos mRNA encoding Xdd1, a mutant form of *Xenopus* Dsh that blocks axis elongation in *Xenopus* and zebrafish (Fig. 4b) (Jessen et al., 2002; Tada and Smith, 2000; Wallingford et al., 2000). Our analysis of division orientation showed that Xdd1 severely disrupts the AV alignment of divisions in all layers of the epiblast (Fig. 3). Cells now divide in a randomized fashion, with spindle orientation almost uniformly distributed from 0 to 90 ^{o} (Compare Fig. 3o, 3p with 3k, 3l). These data are summarized in Fig. 3q and r. In Xdd1-expressing embryos, only about half (55%) of all α angles are within 45 ^{o}, compared with over 90% in the control (Fig. 3q). Similarly, 65% of all β angles are within 45 ^{o} in Xdd1-expressing embryos while the number is over 95% in the control (Fig. 3r). In addition to randomizing division orientation of dorsal epiblast cells, Xdd1 also disrupts their polarity of elongation (LWR = 1.48 ±0.33; Fig. 4e-h; red triangles in 4i). Furthermore, cells divide at random angles rather than perpendicularly to their long axis (Fig. 4k).

Xdd1 disrupts convergence and extension of the dorsal tissue (Jessen et al., 2002; Wallingford et al., 2000) (Fig. 6b). It is thus possible that disruption of oriented division observed in Xdd1 overexpressing embryos was due to compromised morphogenesis of the tissue. To address this, we generated mosaic clones of Xdd1 expressing cells in a wild-type background by injecting a single cleavage stage blastomere. Such embryos undergo normal

morphogenesis, and are indistinguishable from unmanipulated controls morphologically (data not shown). Subsequent analysis shows that these mosaic Xdd1 expressing cells have randomized division orientation, with angular distribution similar to that of embryos overexpressing Xdd1 ubiquitously (Fig. 5c, d). Thus, Dsh exerts its effect on division orientation directly.

Different mutant Dsh constructs have similar effects on division orientation

Dsh is involved in multiple Wnt pathways including the canonical Wnt/ -catenin pathway and the non-canonical pathway related to the *Drosophila* planar cell polarity (PCP) pathway (Fig. 5a) (Veeman et al., 2003a). Xdd1 is a strong inhibitor of PCP signaling, but can block canonical Wnt/ β-catenin signaling in *Xenopus* secondary axis assays (Sokol, 1996; Tada and Smith, 2000). To distinguish between these two pathways, we tested two additional Xdsh constructs: Xdsh-D2 and Xdsh-DEP+ (Fig. 5b) (Rothbacher et al., 2000; Tada and Smith, 2000; Wallingford et al., 2000). Xdsh-D2, which lacks the entire PDZ domain, strongly inhibits PCP but is fully functional for canonical signaling (Rothbacher et al., 2000; Wallingford et al., 2000). Xdsh-DEP+, which only has the DEP domain and lacks the DIX and PDZ domains, blocks PCP and is not functional for canonical signaling (Tada and Smith, 2000).

Analysis of cell divisions in embryos expressing either Xdsh-D2 or Xdsh-DEP+ revealed that division orientation is randomized to a similar extent as caused by Xdd1 (Fig. 5c, d). Therefore, although the three different Dsh deletion constructs can have very different effects on canonical Wnt signaling, they have equivalent ability to inhibit division alignment. This suggests that Dsh controls

division orientation in the dorsal epiblast independently of the canonical Wnt signaling pathway.

Inhibition of the canonical Wnt/β-catenin pathway does not alter division orientation

To further dissect the signaling pathways involved, we functionally blocked the canonical Wnt pathway with two specific antagonists: Dickkopf-1 (Dkk1) (Glinka et al., 1998; Hashimoto et al., 2000; Shinya et al., 2000), and inhibitor of β-catenin and TCF-4 (ICAT) (Graham et al., 2002; Tago et al., 2000). Dkk1 antagonizes Wnt signaling by binding to the lipoprotein receptor-related protein 5/6 (LRP5/6), a possible Wnt co-receptor that is specifically required for canonical Wnt/catenin signaling (Semenov et al., 2001) (Mao et al., 2001) (He et al., 2004). While embryos overexpressing the Dsh constructs exhibit mediolaterally expanded somites, embryos overexpressing zebrafish Dkk1 exhibit a visibly different phenotype with diminished somites and enlarged head (data not shown) (Hashimoto et al., 2000; Shinya et al., 2000), suggesting the major effect of the Dsh constructs is different from that of Dkk1. Significantly, Dkk1 does not affect the AP alignment of divisions (Fig. 5e, f; note the overlap of the control and Dkk1 curves). Similar result is obtained using ICAT, a protein that binds to β-catenin and inhibits its transcriptional function in the canonical Wnt pathway (Fig. 5b). Since uniform overexpression of ICAT during early development interferes with the Nieuwkoop center activity mediated by the maternal canonical Wnt pathway and causes gross dorsal-ventral patterning defects, we generated mosaic clones of ICAT-overexpressing cells on the dorsal

side. The distribution of division orientations in these cells is very similar to that in the control (Fig. 5e, f). Together, these results show that non-canonical Wnt pathway is not involved directly in regulating division orientation during gastrulation.

Loss-of-function of Silberblick/Wnt11 and Strabismus disrupt division orientation

To confirm that PCP signaling regulates oriented cell division in zebrafish, we tested the function of other factors implicated in PCP: Wnt11 and Strabismus (Stbm) (Fig. 5a). Wnt11 is a ligand for the PCP pathway in zebrafish and *Xenopus* (Heisenberg et al., 2000; Tada and Smith, 2000). In our in vivo time-lapse analysis of silberblick (slb)/wnt11 loss-of-function mutants, mitotic divisions in the dorsal epiblast cells exhibit less pronounced AV polarity relative to the control in both the epiblast and perpendicular planes (Fig. 5e, f; compare the red triangles with green circles). The orientation of division in slb mutant embryos is significantly less disrupted than embryos injected with the Dsh reagents (compare Fig. 5e, f with 5c, d), suggesting that additional factors must signal through Dsh to regulate division orientation in the dorsal epiblast. Consistent with this notion, Wnt5a, another non-canonical Wnt, appears to act in parallel with Wnt11 in both zebrafish and *Xenopus* (Du et al., 1995; Kilian et al., 2003; Moon et al., 1993). The function of the PCP pathway was further tested by disrupting Stbm, a transmembrane protein that modulates PCP but does not lie in a linear cascade with Wnt/Dsh (Fig. 4a) (Jessen et al., 2002; Park and Moon, 2002). Following injection with a Stbm morpholino (Park and Moon, 2002),

mitotic divisions in the dorsal epiblast become mis-aligned (blue squares in Fig. 5e, f), revealing an important role for Stbm in this process.

Oriented cell division can be a driving force for axis elongation

Our experiments on the zebrafish dorsal epiblast show both a matching of division orientation and axis elongation normally, and a disruption of oriented cell division and axis elongation following inhibition of PCP signaling. We assessed the contribution of oriented cell division to axis elongation (Fig. 6). Control embryos are well extended by the end of gastrulation, while the Xdd1-expressing embryos have a shorter axis, reaching only 56% of that of the control (Fig. 6a, b, e). On the cellular level, we measured the change in AV dimension that resulted from one round of cell divisions (Fig. 6c, c', d, d'). Oriented division in control embryos increase the AV dimension by 1.5 fold, while randomized divisions in Xdd1-expressing embryos only 1.2, 77% of that in the control (Fig. 6f). This result indicates that oriented cell division accounts for a significant amount, but not all extension of the zebrafish gastrulae. Mediolateral intercalation has been shown to be a driving force for axis elongation in zebrafish and *Xenopus* (Elul and Keller, 2000; Glickman et al., 2003). We propose that oriented cell division and cell intercalation, both under the regulation of the PCP pathway, collaborate to elongate the anterior-posterior body axis in zebrafish. Such a collaborative mechanism may also be employed in axis elongation in the amniotes (Sausedo and Schoenwolf, 1994; Schoenwolf and Alvarez, 1989). We speculate that PCP signaling organizes the cell, orienting both mediolateral intercalation and division axis.

Cell divisions on the ventral side

To gain better understanding of the relationship between tissue elongation and oriented cell division, we studied the division pattern on the ventral side of the embryo, where little tissue elongation takes place. There is a dramatic difference in orientation distribution is dramatic between the dorsal and ventral side of the embryo (Fig. 7). Ventral cells divide in a more randomized fashion, which is aggravated by overexpression of Xdd1. Therefore, there is a correlation between tissue elongation and cell division orientation in different domains of the same embryo.

Discussion

How much does anterior-posterior orientated cell division contribute to axis elongation?

Oriented cell division can contribute to tissue elongation. In this study, we assessed how much anterior-posteriorly oriented cell division can contribute to axis elongation. An unanswered question is whether anterior-posteriorly oriented cell division is required for axis elongation. This is a necessity test, which requires specific disruption of division alignment. This may be achieved by targeting factors affecting orientation of the mitotic spindle. Dynein and dynactin as well as myosin II are potential targets (Ahringer, 2003; Rosenblatt et al., 2004), though disruption of other cellular processes which involve these motor proteins could complicate results (Helfand et al., 2003). Nonetheless, our observations suggest some functions for oriented cell division. During zebrafish gastrulation, cells converge toward the dorsal midline and intercalate at the axial and paraxial region (my own observation) (Glickman et al., 2003). Cell rearrangement happens rapidly and thus could “overpower” division orientation. In the embryo, divisions occasionally occur in non-anterior-posterior orientations. These daughter cells quickly participate in cell movement and their relative positions soon change (my own observation). On the other hand, cell division seems to facility medial-lateral cell rearrangement. As two daughter cells are separating along the anterior-posterior axis, the space between them is inevitably occupied by a neighboring cell (my own observation). Conceivably in this case, the force

for this type of intercalation is created by cell division, and the interacting step requires less force. While the necessity of oriented cell division for axis elongation is not known, medial-laterally oriented cell intercalation combined with anterior-posteriorly oriented cell division is the most productive and energy efficient way to achieve elongation. This combination also allows sloppiness in each mechanism while ensuring the accuracy of the final outcome. After all, for an organism, it is the final outcome that counts.

What is happening along the radial direction?

During gastrulation, another prominent morphogenetic process is epiboly of the entire blastoderm. This process involves thinning of the blastoderm, which, on a cellular level, entails radial intercalation. Our data suggest that oriented division also contributes to the thinning of the blastoderm. Division in the radial direction would increase the thickness of the blastoderm and counter the effect of radial intercalation. Our preliminary data and observation in *Xenopus* (Andrew Ewald, personal communications) show that Wnt/PCP signaling affects blastoderm thinning at gastrulation, or at least at some time points during gastrulation though we did not examine the thickness at completion of epiboly carefully. The blastoderm has a greater thickness when the Wnt/PCP pathway is compromised. However, epiboly proceeds and completes normally in embryos with defective Wnt/PCP signaling. This suggests that thinning of the blastoderm may not be required to drive epiboly (although we cannot rule out the possibility that thinning catches up at some point during epiboly). Redundant mechanisms must exist to ensure the robustness of this important process. Active migration

of blastoderm cells toward the vegetal pole, pulling by the yolk syncytial layer (YSL) or the enveloping layer (EVL) are all possibilities. That the blastoderm cells are loosely associated with the EVL and these two layers move relative to each other makes pulling by the EVL unlikely (our observations).

How does spindle align with the anterior-posterior axis?

In this study, we used H2B-GFP to mark the chromosomes of the cells. In some cells, we observed the metaphase chromosomes which collectively appear as a small rod due to their arrangement, rotate before being separated into the daughter cells. This suggests that the spindle rotates during metaphase during oriented cell division. Examining behaviors of the spindle is the subject of Chapter 3.

Conclusions

Our results demonstrate the importance of non-canonical Wnt/PCP signaling in controlling cell division orientation and axis elongation in the early zebrafish embryo. Given that the PCP pathway has been shown to regulate spindle orientation during asymmetric cell division in *C. elegans* and *Drosophila* (Gho and Schweisguth, 1998; Schlesinger et al., 1999), our findings suggest that it plays an evolutionarily conserved role in vertebrates. Oriented cell division is a common feature of many vertebrate developmental processes, ranging from the generation of cell layers (Chalmers et al., 2003), to primitive streak extension (Wei and Mikawa, 2000) and neurogenesis (Das et al., 2003). An interesting and testable possibility is that these processes have a similar dependence on PCP signaling. Together with our existing knowledge of the various roles of PCP signaling, our results highlight the central nature of the PCP pathway in regulating the multiple mechanisms that generate the elongation of the vertebrate embryo in its early development.

Acknowledgements

We thank Masahiko Hibi (Zdkk1), Maiyon Park (Stbm MO), John Wallingford (Xdsh-D2), Reinhard Köster (H2B-GFP), Sean Megason (H2B-RFP1 and memRFP1), Masazumi Tada (Xdsh-ΔPDZ and Xdsh-DEP+), Helen McBride (ICAT) for providing the plasmids and morpholino, and Carl-Philipp Heisenberg for the silberblick/wnt11 mutants. We thank Sujata Bhattacharyya, Marianne Bronner-Fraser, Martin Garcia-Castro, David Koos, Reinhard Köster, Brian Link, Sean Megason and John Wallingford for stimulating discussion and critical reading of the manuscript.

Figure 2-1 Nuclei marked by H2B-GFP

Different cell layers can be distinguished by the size and relative movement of the nuclei. a-e are images of increasingly deeper focal planes from the same embryo. Cells in the superficial enveloping layer, or EVL, are easily distinguished by their large and flat nuclei (arrows in a and b). The yolk syncytial layer, or YSL, also have large nuclei (double arrowheads in d and e). The deep cells have small nuclei (arrowheads in a, b, and d; panel c). Scale bar=25 μm.

Figure 2-1 Nuclei marked by H2B-GFP

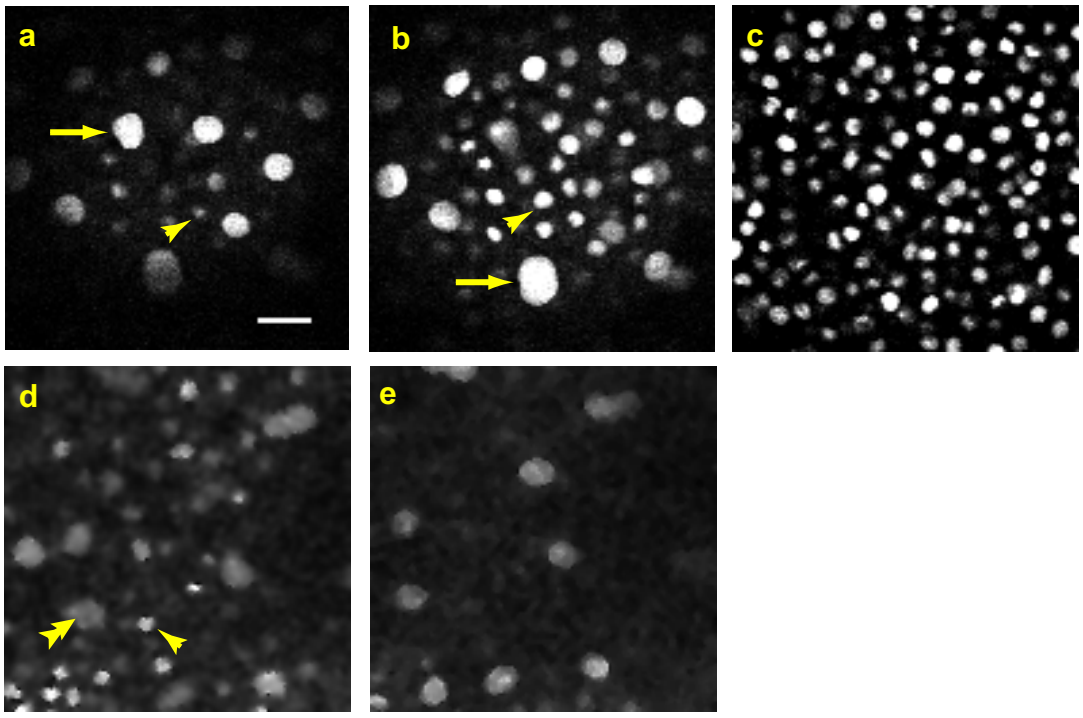

Figure 2-2 Imaging and data analysis methods

a, Embryos are injected with various constructs, raised to early gastrula stage and cultured on the microscope stage for collection of 4D (x, y, z, t) images. b, Top, images of the dorsal region (shaded) are analyzed for cell division orientation. Embryo curvature can be ignored for the small region selected. The AV axis corresponds to the x axis, ML to y and depth to z of the image sets. A pair of daughter nuclei is shown as green spheres. The line connecting the pair is projected onto the xy plane and the zy plane. α represents the angle between the projection and the y axis in the xy plane, and β in the ZY plane. Bottom, schematics illustrating α and β within the whole embryo. dm, dorsal midline; eq, equator.

Figure 2-2 Imaging and data analysis methods

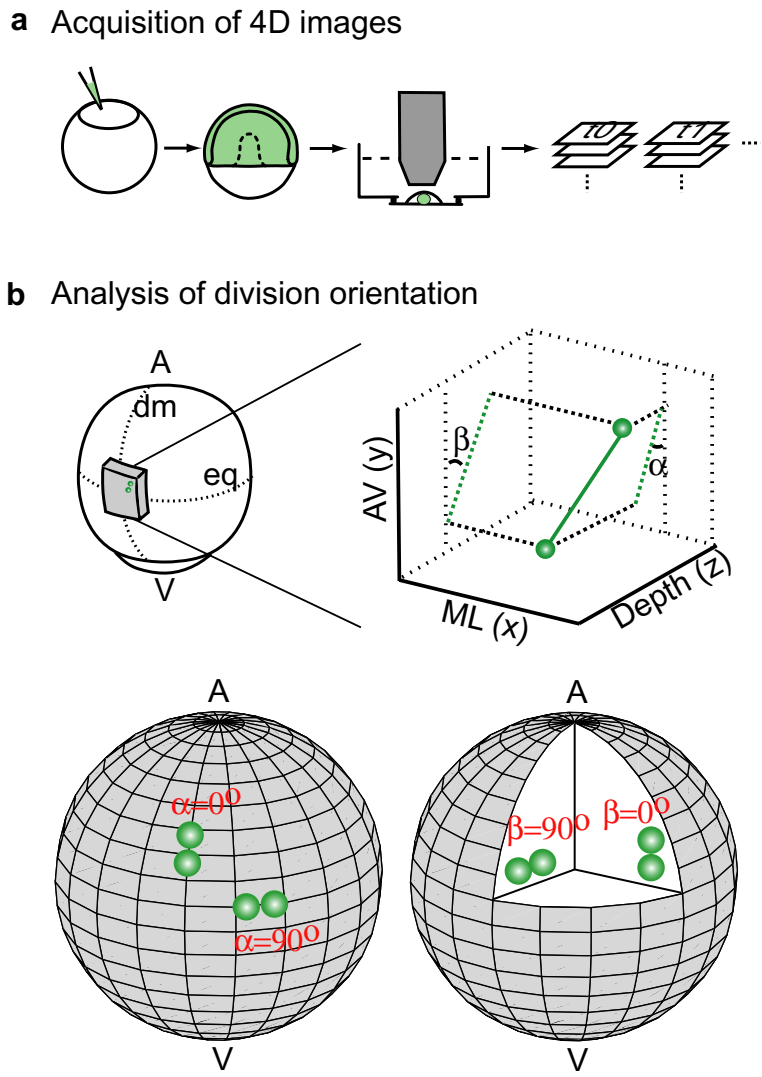

Figure 2-3 Xdd1 randomizes division orientation in zebrafish dorsal epiblast

a-h are confocal time lapse images from a representative control (a-d and a'-d') and Xdd1-expressing (e-h and e'-h') embryo. a-d and e-h are xy, a'-d' and e'-h' are yz cross-sections, respectively. Dividing nuclei are highlighted in green (shown in xy view only) or red (shown in both xy and yz views). Divisions are aligned with the AV axis in the control but random in the Xdd1-expressing embryo. Animal pole is up in these images. Time interval is 2.1 minutes for the control and 1.9 minutes for Xdd1. Scale bar, 20 μm. All divisions in the dorsal region are plotted as lines in i-j (control) and m-n (Xdd1). Most lines are AV oriented in the control but randomly oriented in the Xdd1-expressing embryo. k-l and o-p, Histograms showing the α and β angles between the division axis and AV axis in the control (k-l) and Xdd1-expressing (o-p) embryo. Most angles are close to 0 ^{o} in the control embryo but are distributed rather uniformly from 0 to 90 ^{o} in the Xdd1-expressing embryo. q-r, Cumulative plots of division angles using 45 ^{o} as the cut-off. Values plotted are mean ± SD (Control, 521 divisions/4 embryos. Xdd1, 533 divisions/3 embryos).

Figure 2-3 Xdd1 randomizes division orientation in the dorsal epiblast

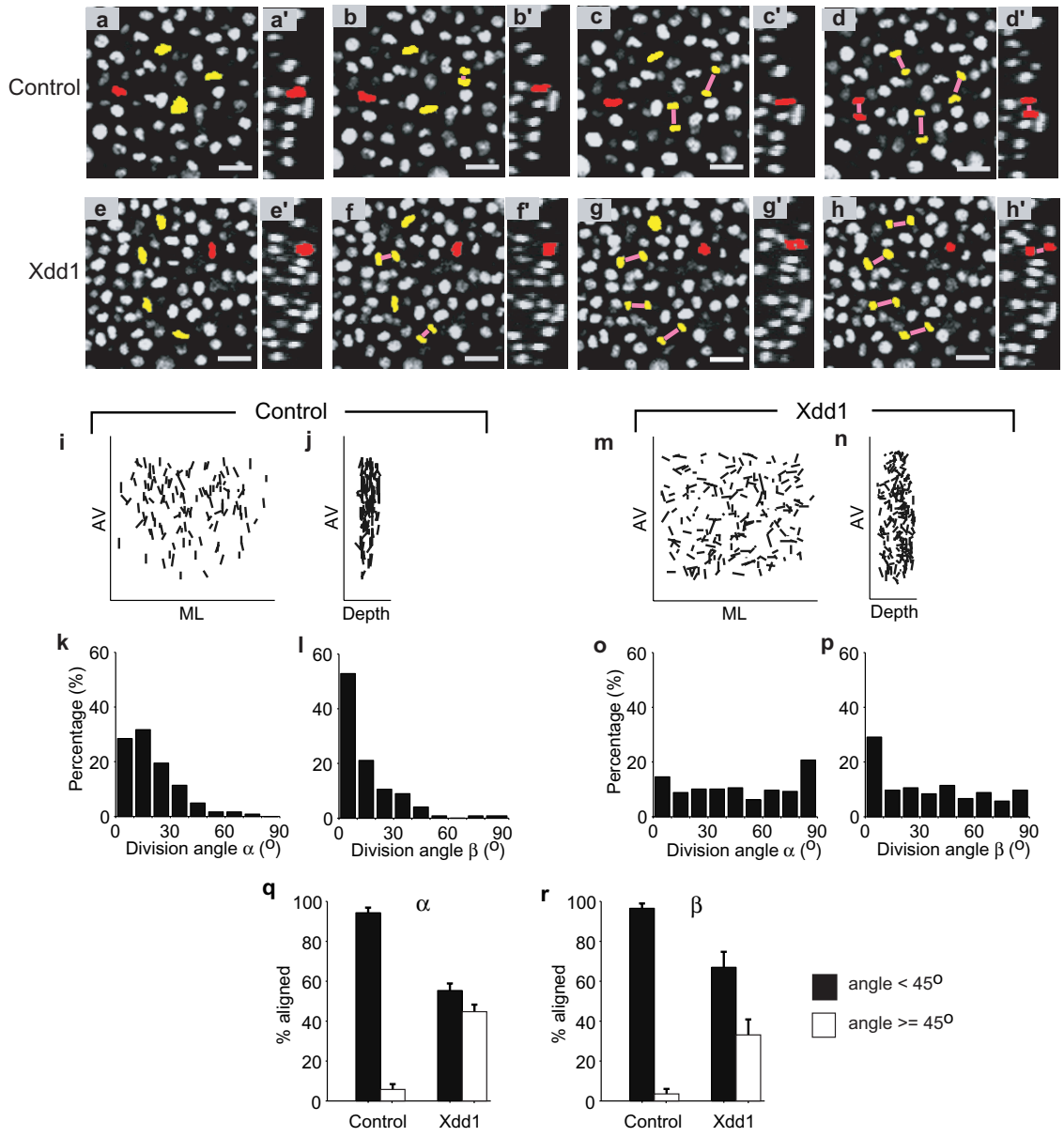

Figure 2-4 Relationship between cell elongation and division orientations

a-h, Confocal time lapse images from a typical control (a-d) and Xdd1-expressing (e-h) embryo double-labeled with membrane RFP (red) and H2B-GFP (green). Dividing cells are marked by arrows. Time interval is 2 minutes. Scale bar, 20 μm. i, Cumulative plot of cell elongation orientation with respect to the AV axis. Control cells (green circles) elongate mediolaterally, indicated by the concave shape the cumulative plot. This polarity is disrupted in Xdd1-expressing cells (red triangles), thus the cumulative plot approximates a straight line whose slope is 1. j, Cumulative plot of cell division orientation with respect to the AV axis, showing randomized orientation caused by expression of Xdd1. k, Cumulative plot of the angle between a cell's elongation axis and division axis. The 90 ^{o} correlation shown by the control cells are not observed in Xdd1-expressing cells. (Control, 192 cells/3 embryos; Xdd1, 184 cells/3 embryos.)

Figure 2-4 Relationship between cell elongation and division orientations

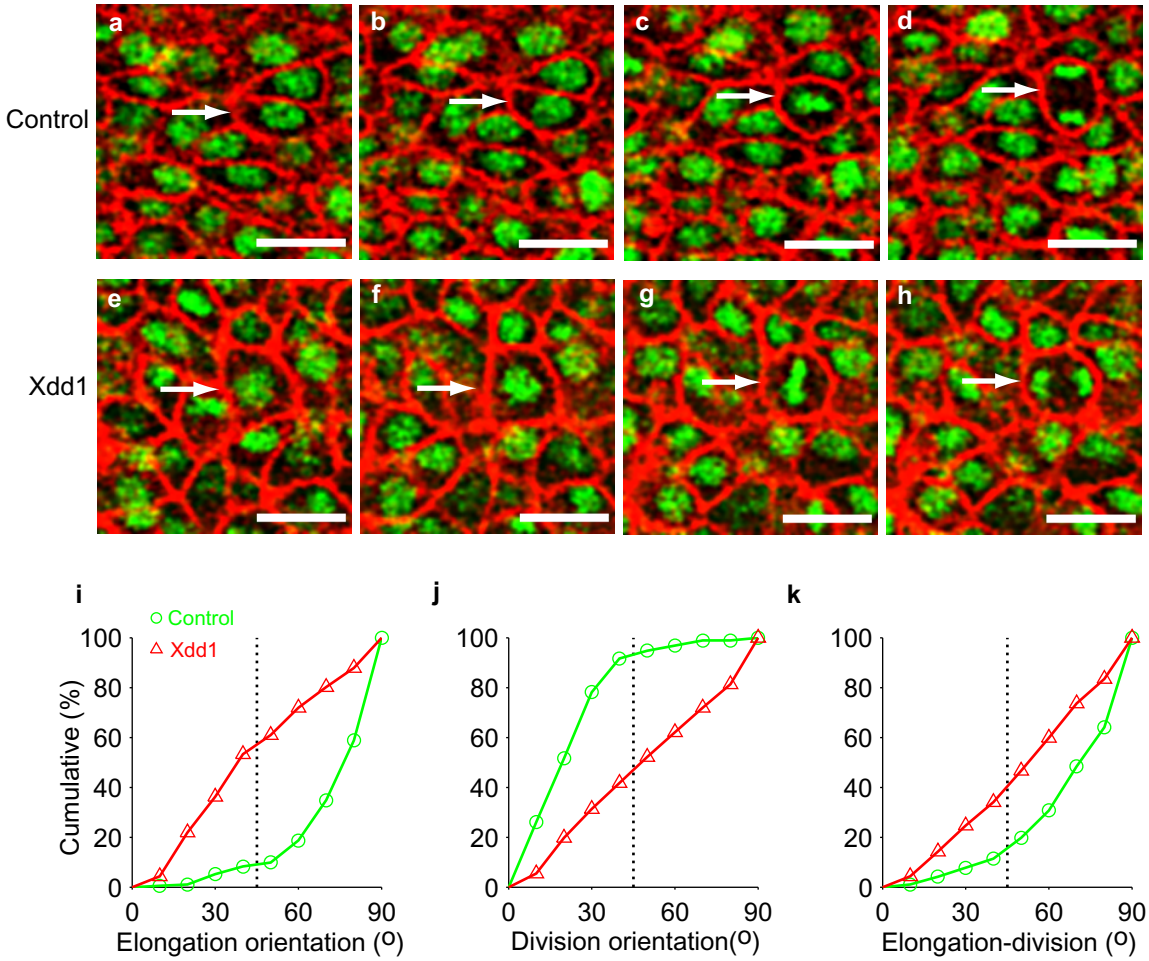

Figure 2-5 Components of the PCP pathway regulate division orientation

a, Diagram of the vertebrate PCP and canonical Wnt pathways. b, Different Dsh constructs tested. c-d, Cumulative plots of division angles from embryos expressing various Dsh constructs. Xdd1, Xdsh-D2 and Xdsh-DEP+ disrupt division orientation polarity to a similar degree. Xdd1 mos: Xdd1 mosaic clones in wild-type backgrounds. The dotted lines represent 45 o thresholds. (Control, 521 divisions/4 embryos; Xdd1, 533 divisions/3 embryos; Xdsh-D2, 378 divisions/2 embryos; Xdsh-DEP+, 555 divisions/3 embryos. Xdd1 mos, 138 divisions/6 embryos.) e-f, Cumulative plots of division angles from embryos in which different canonical Wnt or PCP pathway components are compromised. Mutation in the slb/wnt11 gene and knock-down of Stbm by a morpholino both randomize division orientations. Neither Dkk1 nor ICAT affects the orientation distribution significantly. (slb, 411 divisions/3 embryos; Stbm MO, 638 divisions/4 embryos; Dkk1, 500 divisions/5 embryos; ICAT 106 divisions/6 embryos.)

Figure 2-5 Components of the PCP pathway regulate division orientation

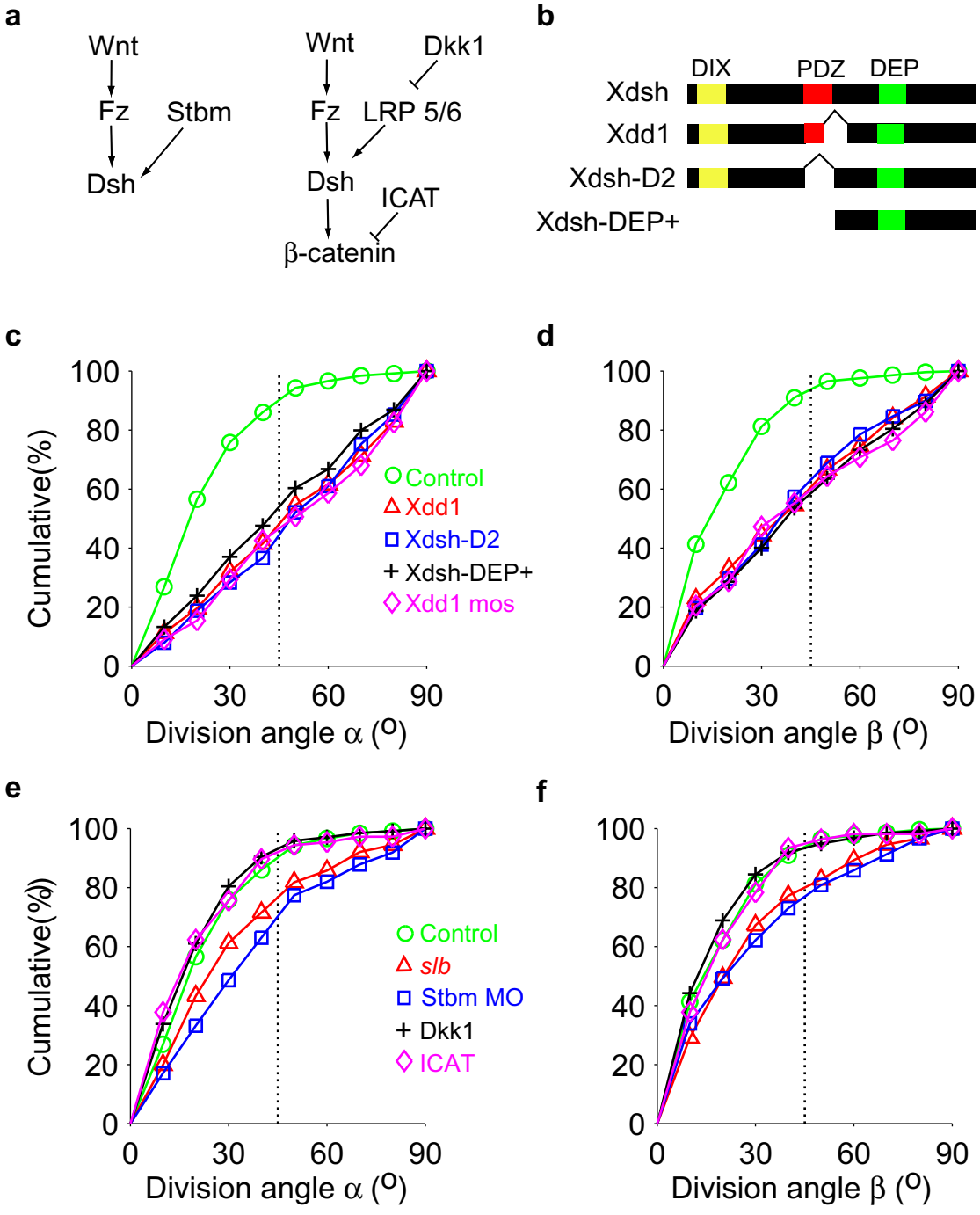

Figure 2-6 Contribution of oriented cell division to axis elongation

A tail-bud stage control embryo has a well extended body axis (a), but an Xdd1 expressing embryo has a significantly shorter axis (b). Asterisks mark the anterior and posterior limits of the body axis. c-d', The AV dimension of a daughter cell pair after cytokinesis (marked by white lines) was measured and normalized by dividing the AV dimension of the mother cell (white arrows) at metaphase. c and c' are control, and d and d' are Xdd1-expressing cells. e, Relative extension of overall body axis in Xdd1-expressing embryos (n=11) compared with controls (n=11). f, Relative extension resulted from cell divisions in Xdd1-expressing embryos (n=41 cells/2embryos) compared with controls (n=46 cells/2 embryos). All values shown in e and f are mean ± SD.

Figure 2-6 Contribution of oriented cell division to axis elongation

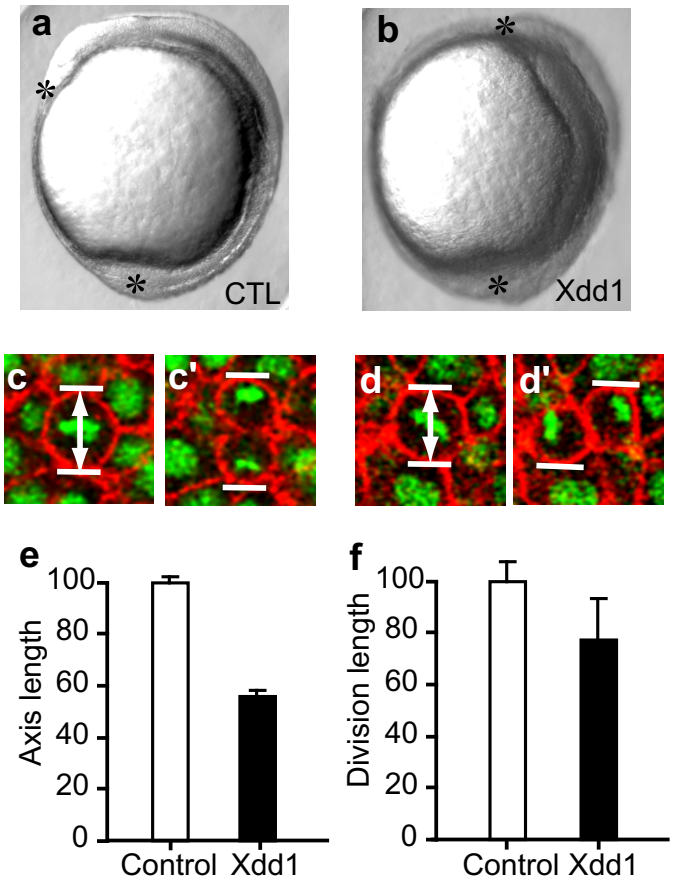

Figure 2-7 Distribution of mitotic division orientations on the dorsal and ventral sides

a, Cumulative plot of division angles α. b, Cumulative plot of division angles β. Mitotic divisions are well aligned with respect to the AV axis on the dorsal side in wild-type embryos (WT dor). By comparison, divisions on the ventral side of the embryo exhibit only minor bias towards the AV axis (WT ven). This bias in orientation distribution is disrupted by misexpression of Xdd1 mRNA. (WT dor, 192 divisions/3 animals; WT ven, 271 divisions/3 animals; xdd1 ven, 198 divisions/2 animals.)

Figure 2-7 Distribution of mitotic division orientation on the dorsal and ventral sides

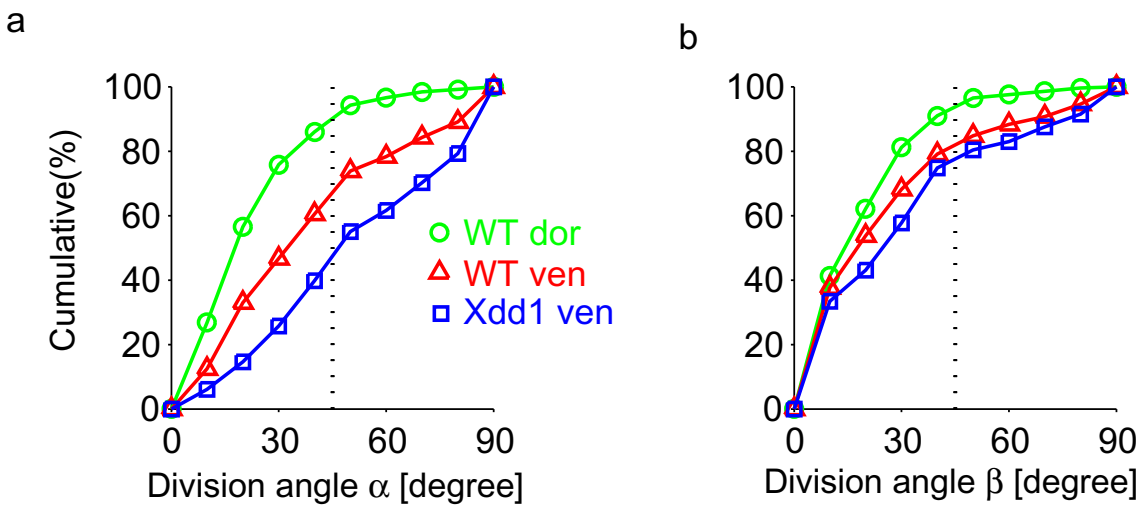

Chapter 3

Spindle dynamics during orientated cell division in zebrafish

Introduction

In many cells, mitotic division often occurs along a specific orientation. Oriented cell divisions play important roles in cell morphogenesis, asymmetric segregation of fate determinants, and embryogenesis. Mechanisms underlying oriented divisions are studied extensively in *Saccharomyces cerevisiae* (Nelson, 2003; Schuyler and Pellman, 2001), *Caenorhabditis elegans* (Schneider and Bowerman, 2003), and *Drosophila melanogaster* (Bardin et al., 2004; Chia and Yang, 2002; Jan and Jan, 2001). But our understanding of these processes in vertebrates is limited.

The process of oriented cell division can divided into three steps. First, the unpolarized cell receives a directional external signal (or signals), which could be as diverse as ligand binding (diffusible or membrane-bound), gravity, mechanical force, electrical current, or sperm entry. Second, the external polarizing signal impinges on the cell, creating polarity within the cell. This step typically involves formation of asymmetrically localized (or activated) “polarity complexes”. Third, the polarity complexes impinge on downstream cellular machinery that aligns the mitotic spindle along a polarity axis. Mitotic spindle polarity is only one readout of cell polarity. The polarity signal can be relayed to a number of other modular cellular machineries to effect changes in cell behaviors. This could be localization of cell fate determinants, changes in cell morphology, or activation of signaling cascades.

During the development of the *Drosophila* nervous system, each sensory organ precursor cell (SOP) divides along the anterior-posterior axis within the

epithelial plane to generate an anterior pIIb cell and a posterior pIIa cell (Gho and Schweisguth, 1998). The anterior-posterior polarity requires the planar cell polarity (PCP) components Frizzled, Dishevelled, Flamingo, and Strabismus (Bellaiche et al., 2004; Gho and Schweisguth, 1998; Lu et al., 1999). The anterior-posterior orientation of the mitotic spindle is a result of centrosomal rotation from random initial positions. In another type of neural precursors, the neuroblasts, asymmetric division is perpendicular to the epithelial plane, along the apical-basal axis (Kraut et al., 1996). This polarity does not require the PCP genes, but a gene called *inscuteable*. The centrosomes initially line up within the epithelial plane, and rotate by 90^{o} to align with the apical-basal axis (Kaltschmidt et al., 2000). In both SOPs and neuroblasts, rotation starts after the two centrosomes separate to two opposite poles but before spindle formation, and continues after spindle formation.

Our previous work, which is described in Chapter 2 of this thesis, shows that mitotic divisions are preferably aligned with the anterior-posterior axis in axial tissues during zebrafish gastrulation. This polarity, playing a role in elongation of the anterior-posterior axis, depends on components of the non-canonical Wnt/PCP pathway. When the function of the Wnt/PCP pathway is compromised, orientation of mitotic divisions becomes randomized with respect to the anterior-posterior axis. In that study, we followed divisions using chromosomal marker Histone2B-GFP, and therefore we did not know how alignment of the mitotic spindle with the anterior-posterior axis takes place.

To better understand behaviors of the mitotic spindle during orientated cell division, we marked microtubules with GFP and followed their behaviors in vivo using time-lapse microscopy. We found that the spindle forms at random orientations and rotates to line up with the anterior-posterior axis. Disruption of the PCP pathway using the mutant form of Dishevelled, Xdd1, does not abolish the spindle's ability to rotate, but the ability to line up with the anterior-posterior axis. These findings have two implications: First, the polarity cues leading to anterior-posteriorly oriented division are established or read out during mitosis. Second, Dishevelled may be part of the polarity cue complex.

Methods

Constructs

The pEGFP-tub construct is commercial available from Clontech. The fragment containing the human α-tubulin coding region fused to the C-terminus of EGFP was excised using NheI and BamHI. The fragment was blunted and subcloned into the StuI site of pCS2+.

The Xdd1 construct (in pCS2+) is obtained from M. Tada (Tada and Smith, 2000).

mRNA synthesis and injection

mRNA was synthesized with the eMessage eMachine kit from Ambion (Austin, TX). Concentration used for injection is 0.3 μg/μl for α-tubulin-GFP, and 0.5 μg/μl for Xdd1. Less than 1 nl of mRNA was injected into the blastomeres of one-cell stage embryos.

Confocal time-lapse imaging

Control or Xdd1-overexpressing embryos were raised to embryonic shield stage. Embryos were dechorionated and mounted in 1.3% low gelling point agarose in a Labtek chamber slide with a number 1 coverslip bottom. Four-dimensional (4D) confocal time-lapse imaging was carried out on an inverted Zeiss LSM 510 laser scanning microscope, using a 40x/1.2NA C-Apochromat water immersion objective. z-stacks were collected at 20-second intervals and spacing between consecutive z slices was set to values recommended by the

microscope controlling software (typically around 1.7 μm). Embryos were imaged for 3.5 to 4 hours to approximately bud stage. The 488 nm laser line was used for imaging GFP. Low laser power was used to minimize phototoxicity. Development of each embryo was monitored after the imaging session and embryos showing abnormal necrosis were not included for analysis.

Results

α-tubulin-GFP reveals changes in microtubule organization during the cell cycle

To visualize mitotic spindles, I imaged embryos expressing the α-tubulin-GFP fusion protein. Distribution and intensity of the GFP signal change during the cell cycle due to changes in microtubule organization (Fig. 1 to Fig. 6). At interphase, the GFP signal is uniformly distributed in the cytoplasm and the nuclei appear as dark circles. During mitosis, the GFP signal becomes more concentrated to the mitotic apparatus. Towards the end of cytokinesis, the GFP signal reveals the midbody, appearing as a buddle of microtubules that persist for over 10 minutes after cytokinesis (Fig. 1 t=12:20 to t=14:20 and data not shown).

It takes approximately 12 minutes to finish cytokinesis from the time of centrosome duplication.

Oriented cell division depends on rotation of the mitotic spindle towards the anterior-posterior axis

Dorsal epiblast cells divide along the anterior-posterior axis of the embryo (Chapter 2). This requires the mitotic spindle to line up with anterior-posterior axis before anaphase. To understand how this happens, I examined centrosome and spindle behaviors during oriented division.

The duplicated centrosomes can be detected as early as 4 minutes before spindle starts to form (Fig. 1, t=0:00). The centrosomes appear as two closely-

spaced dots at variable positions at the periphery of the nucleus. They become brighter and larger as mitosis progresses, presumably as their associated asters grow denser and larger.

Subsequently, the two centrosomes migrate around the nucleus towards opposite poles of the cell. In the cell depicted in Fig.1, one centrosome appears to be closer to the nucleus and start migration before the other one. This phenomenon was also observed in mitosis of the pI cell in *Drosophila* (Bellaiche et al., 2001a).

After reaching opposite poles, the centrosomes stop and organize the formation of the spindle. The axis joining the two centrosomes and thus the newly formed spindle is randomly oriented with respect to the anterior-posterior axis. The spindle can occupy a parallel (Fig. 1), perpendicular (Fig. 2), or intermediate position to the anterior-posterior axis. The spindle's initial position is not limited to the blastoderm plane. For example, in the cell depicted in Fig. 3, the spindle forms initially at an angle to the XY plane (the spindle is clearly visible at t=0:20). The nuclear envelop breaks down at approximately the same time as when the centrosomes stop migrating (Fig. 1, t=3:40 and Fig. 2, t=1:20).

Spindles that set up parallel to the anterior-posterior axis do not show significant movement before separation of their two poles at anaphase (Fig. 1). The spindles, however, are not stationary. Instead, they tend to seesaw at the vicinity of the anterior-posterior axis (compare t=6:20 with 6:00, and t=8:00 with 7:20).

By comparison, spindles forming at an angle to the anterior-posterior axis rotate to line up with the anterior-posterior axis (Fig. 2 and 3). Each rotation occurs by the shortest path such that the angle between the starting and ending positions does not exceed 90^{o} (n>100 in three animals). The more anterior spindle pole moves toward the anterior end of the anterior-posterior axis while the more posterior spindle pole moves toward the posterior end of the anterior-posterior axis (t=3:00 to 6:40 in Fig. 2; t=0:40 to t=2:40 in Fig. 3). Frequently, the spindle "overshoots" (t=6:00 in Fig. 2) and then rotates back (t=6:40 in Fig. 2). In addition, spindle rotation is not restricted to any plane but is three-dimensional. This is best illustrated in Fig. 3, which shows rotation in the YZ and XY planes.

The above results indicate that oriented cell division we previously characterized during zebrafish gastrulation is mediated by rotation of the mitotic spindle before anaphase.

Dishevelled regulates the direction of spindle rotation

Non-canonical Wnt/PCP signaling is required for aligning cell divisions along the anterior-posterior axis. To understand how this pathway regulates behaviors of the mitotic spindle, I imaged embryo co-expressing Xdd1, a mutant form of *Xenopus* Dsh that disrupts the signaling through the Wnt/PCP pathway (Chapter 2). As in cells in control embryos, centrosomes form at various positions around the nucleus in Xdd1 expressing cells, migrate to opposite poles and form the spindle along a random axis. The spindles also rotate during metaphase. However, the rotations do not result in alignment of the spindles with the anterior-posterior axis. In the cell depicted in Fig. 4, the spindle initially

forms along the anterior-posterior axis. It then rotates counterclockwise and settles into an orientation perpendicular to the anterior-posterior axis. In another case depicted in Fig. 5, the spindle forms at an angle to the anterior-posterior axis. Subsequently, it rotates clockwise and stops at roughly a 60^{o} angle with respect to the anterior-posterior axis. In a few cells, the spindle is observed to rotate more than 90^{o}, a phenomenon not observed in control cells (data not shown).

Discussion

In oriented division in the zebrafish gastrula, the mitotic spindle is aligned with the anterior-posterior axis. To understand the cell biology of this polarity event, I studied the spindle dynamics in cells undergoing oriented cell division using time-lapse microscopy.

I found that the mitotic spindle sets up at a random orientation, and then rotates to line up with the anterior-posterior axis. In Xdd1 overexpressing cells, which divide at random orientations, the spindle still has the ability to rotate. But instead of rotating to line up with the anterior-posterior axis, the spindle stops at a random end position. Spindle rotation seems to be a conserved mechanism in establishing division orientation. In *Drosophila* neuroblasts and SOPs, final spindle orientation is established by rotation of the spindle (Bellaiche et al., 2001a; Kaltschmidt et al., 2000; Roegiers et al., 2001).

Is Dsh part of a polarity complex in oriented cell division?

Oriented cell division involves three steps of regulation: 1) receiving polarizing signal, 2) establishing polarity within the cell by forming polarity complexes, and 3) relaying polarity information to downstream cellular machinery that aligns the mitotic spindle.

How does Dsh exert it function in this process? Multiple lines of evidence suggest that Dsh may be part of the cellular polarity complex. First, my finding that Dsh is not required for the spindle rotation per se, but dictates the end position of spindle rotation, suggests that Dsh is not part of the downstream

machinery but instead is involved in setting up the polarity. Second, in *Drosophila*, Dsh is required for planar cell polarity in multiple contexts, including the wing, eye and sensory organ precursors (SOPs) (McNeill, 2002; Strutt, 2003). Dsh is part of a core polarity complex that is asymmetrically localized within the cells of the wing and eye (Axelrod, 2001; Shimada et al., 2001; Strutt et al., 2002). Although the subcellular localization of Dsh has not been directly looked at in the SOPs, Frizzled has been shown to asymmetrically localize in this case (Bellaiche et al., 2004; Bellaiche et al., 2001b). Moreover, there is also evidence that Dsh shows subcellular localization in vertebrates. In *Xenopus* dorsal mesoderm explants undergoing convergent extension, Dsh can be observed to accumulate at the medial-lateral ends of elongated cells (Kinoshita et al., 2003).

By analogy, in zebrafish oriented divisions, Dsh could also be localized to the medial-lateral ends of the cells while spindles line up with the anterior-posterior orientation. If this were the case, Dsh (and other members of the polarity complex) would work in a different way than in other systems such as *C. elegans* and *Drosophila* where the spindle lines up with the polarity complex. Dsh would “repel” instead of “attract” spindle poles. Whether Dsh localize to the medial-lateral cortex to repel or the anterior-posterior cortex to attract spindle, a persistent localization throughout interphase and mitosis may not be true. As discussed below, the polarity axis guiding spindle orientation appear to be established during mitosis.

Alternatively, Dsh could accumulate at the medial-lateral ends during interphase and at the anterior-posterior ends during mitosis. During interphase, it

is responsible for cell elongation and generation of protrusions along the medial-lateral direction, while during mitosis, it directs mitotic spindle rotation. This is a wild speculation since it is not intuitive to conjure up a way that could lead to the switching of the polarity axis in our system. Cell division is not synchronous during zebrafish gastrulation, and thus those at interphase and those undergoing mitosis are intermixed with each other. In other words, mitotic and interphase cells are not spatially and temporally separable, which makes polarity switching an unlikely mechanism.

Dsh could also act permissively. It may be uniformly localized around the cortex and acts as an adaptor for the “real” polarity proteins. It needs to be noted medial-lateral localization of Dsh was observed in extremely elongated *Xenopus* cells (Kinoshita et al., 2003). Thus it is possible this pattern of Dsh localization may not be true in cells undergoing oriented division in zebrafish, which are not significantly elongated. To distinguish between these possibilities, high resolution imaging studies of Dsh localization is necessary.

What is the downstream machinery for spindle rotation and positioning?

Studies in a number of organisms show that spindle positioning involves interactions of microtubules with the cell cortex (Gonczy, 2002). In the budding yeast, spindle positioning relative to the mother-bud polarity axis involves two machineries that underlie different stages of the process, but are partially overlapping (Schuyler and Pellman, 2001). Loss of both machineries disrupts spindle orientation and causes lethality. The first machinery depends on the APC homolog Kar9, EB1 homolog Bim1 and type V myosin Myo2, and is

responsible for the initial movement of the nucleus toward the bud neck and the alignment of the spindle along the mother-bud axis. In this process, Kar9 is localized to only one of the spindle pole bodies (Liakopoulos et al., 2003) where it is linked to microtubules with Bim1 (Korinek et al., 2000; Lee et al., 2000; Miller et al., 2000). Kar9 then migrates along the astral microtubules towards the plus ends (Liakopoulos et al., 2003). There it binds to the tail of the actin motor Myo2 (Yin et al., 2000), which moves Kar9 and the plus-ends of the microtubules to the bud tip, along polarized actin cables (Hwang et al., 2003; Liakopoulos et al., 2003). Consequently, the spindle is aligned along the mother-bud axis. It is not known whether and how microtubules interact with the bud tip. Homologues of Kar9 and Bim1, APC and EB1 are required for spindle positioning in neuroepithelial cells in *Drosophila* (Lu et al., 2001).

The second machinery involves dynein and dynactin, and is responsible for inserting the spindle and nucleus into the bud neck. Dynein (and possibly dynactin) accumulates at microtubule plus ends (Lee et al., 2003; Sheeman et al., 2003). A possible mechanism is that dynein is anchored to the bud tip via an anchor protein and moves toward the minus end of the microtubule. Since the bud tip is fixed, this pulls the microtubules and thus the nucleus toward the bud tip. Requirement for dynein and dynactin has also been established in other systems, including spindle rotation in the *C. elegans* zygote, spindle orientation in *Drosophila* germline stem cells, and spindle orientation in mammalian epithelial cells (Ahringer, 2003).

How does Dsh regulate the downstream machinery to effect stereotyped spindle rotation?

The Dsh polarity complex could cause spindle rotation in two mechanisms. First, it can recruit microtubule anchors than capture astral microtubule ends in a search-and-capture process. Second, it can cause polarized actin polymerization along the polarity axis (in this case along the anterior-posterior axis). The astral microtubule ends can be transported along the actin tracks towards the anterior-posterior poles. Both models have been proposed in the budding yeast (Gundersen and Bretscher, 2003).

In *Drosophila* neuroblasts and SOPs, and in *C. elegans* zygote, heterotrimeric G proteins are important to transduce the polarity cues to the mitotic spindle. In *Drosophila*, the Gα subunit is associated with partner of inscuteable, a member of the polarity complex (Chia and Yang, 2002). The G protein themselves do not participate in overall cell polarity establishment but affect the position of the spindle. Functional mechanisms are not known because so far no targets have been identified for these G proteins. Interestingly, heterotrimeric G proteins are also involved in regulating convergence and extension downstream of Wnt11 in *Xenopus* (Penzo-Mendez et al., 2003). It is thus likely G proteins are used to orient the spindle in vertebrates.

Coupling polarity with cell cycle progression

Polarity needs to be tightly coupled to cell cycle progression. In our system, the observation that the mitotic spindle forms at a random orientation

and then rotates to align with the anterior-posterior axis indicates that spindle orientation is specified after prophase. This suggests that the polarity cues may become established after the onset of mitosis, probably after spindle formation. The seesawing of the spindle may reflect the completion of polarity cue localization. Alternatively, polarity could be established earlier, but the downstream machinery rotating the spindle only becomes active later during mitosis. Studying the temporal correlation of polarity complex formation and spindle dynamics will offer help distinguish these two possible mechanisms.

Polarity during neurulation

Previous studies and our preliminary data show that divisions at the midline of the neural keel are medial-laterally aligned while divisions at other regions are not aligned (Concha and Adams, 1998; Kimmel et al., 1994; Papan and Campos-Ortega, 1994). The medial-lateral divisions separate daughter cells across the dorsal midline. The functional significance of this process for the embryo remains a mystery. How does spindle in these midline cells become aligned to a perpendicular axis? Does this event require the Wnt/PCP pathway? What is the localization pattern of the PCP components? What are the behaviors of the centrosomes and spindle? How does division polarity in the lateral cells lost? There are many unanswered questions.

Figure 3-1 Centrosome movement and spindle dynamics in a wild-type dorsal epiblast cell during gastrulation

Microtubules are revealed by α-tubulin-GFP. The anterior-posterior axis is along the diagonal of the images with anterior to the upper right. Before nuclear envelope breakdown, the nucleus appears as a dark sphere (asterisk in t=0:00 and corresponding structures in subsequent frames). Centrosomes can be detected by their associated asters, starting from 4 minutes before spindle formation (arrowheads, t=0:00 and onwards). The duplicated centrosomes separate and migrate around the nucleus toward opposite poles (t=1:20 and onward). After reaching opposite poles, the centrosomes send out microtubules to form the spindle (t=4:20). The spindle is set up roughly along the anterior-posterior axis and seesaws around the axis (rotation is visible from t= 6:00 to t=6:20, and from t=7:20 to t=8:00). α-tubulin-GFP accumulates to the midbody at the end of cytokinesis, and persists after two daughter cells have separated (arrows in t=11:20 onwards). Time is in minute. Scale bar=6 μm.

Figure 3-1 Centrosome movement and spindle dynamics in a wild-type dorsal epiblast cell during gastrulation

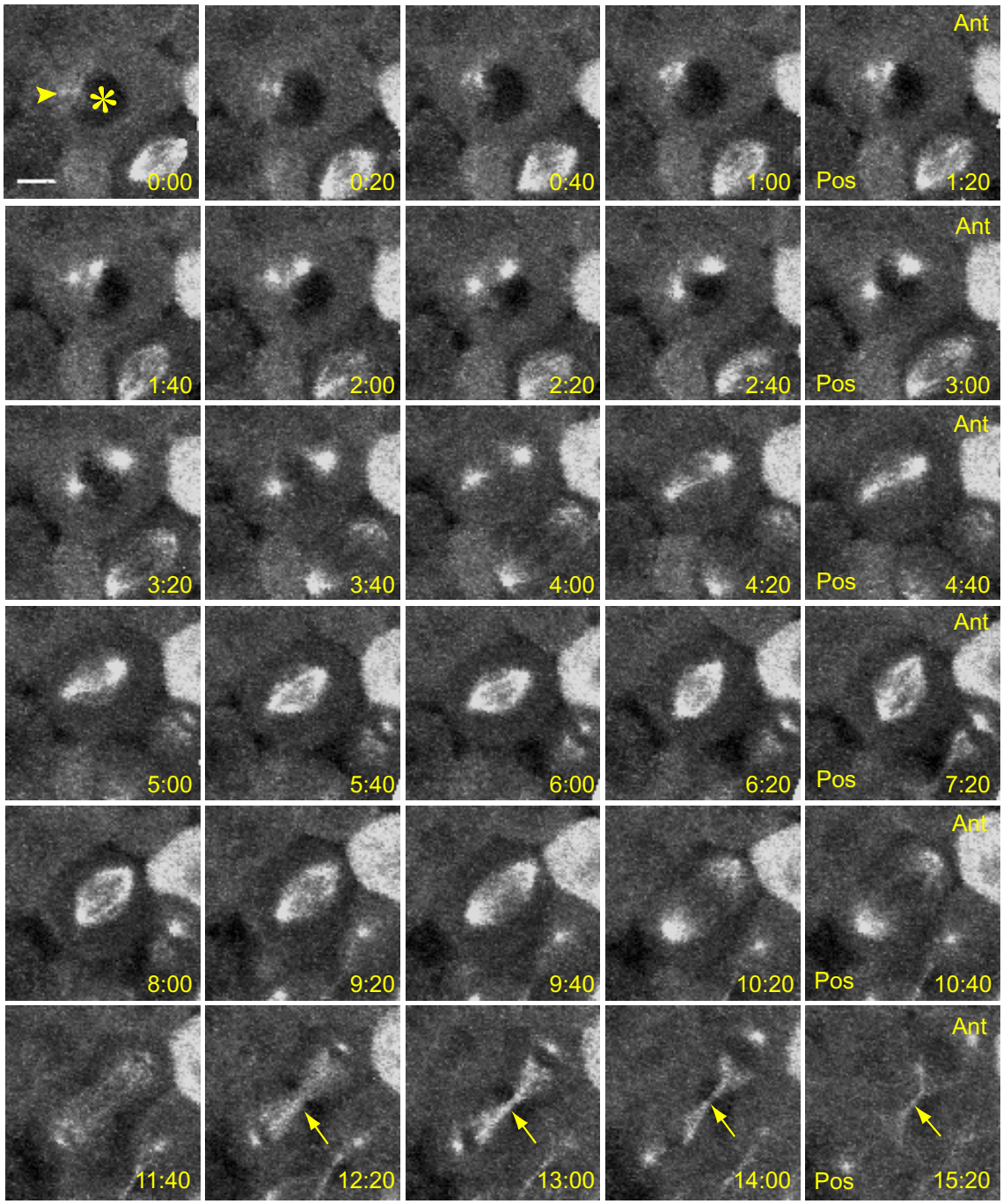

Figure 3-2 Spindle reorients during mitosis in the dorsal epiblast

Microtubules are revealed by α-tubulin-GFP in a wild-type gastrula. The anterior-posterior axis is along the diagonal of the images with anterior to the upper right. This spindle forms perpendicularly to the anterior-posterior axis (t=3:00). It rotates by nearly 90^{o} to line up with the anterior-posterior axis (from t=3:20 to t=6:40) during metaphase. During rotation, the spindle overshoots (t=6:00) and then rotates back (6=6:40). Time is in minutes. Scale bar=6 μm.

Figure 3-2 Spindle reorients during mitosis in the dorsal epiblast

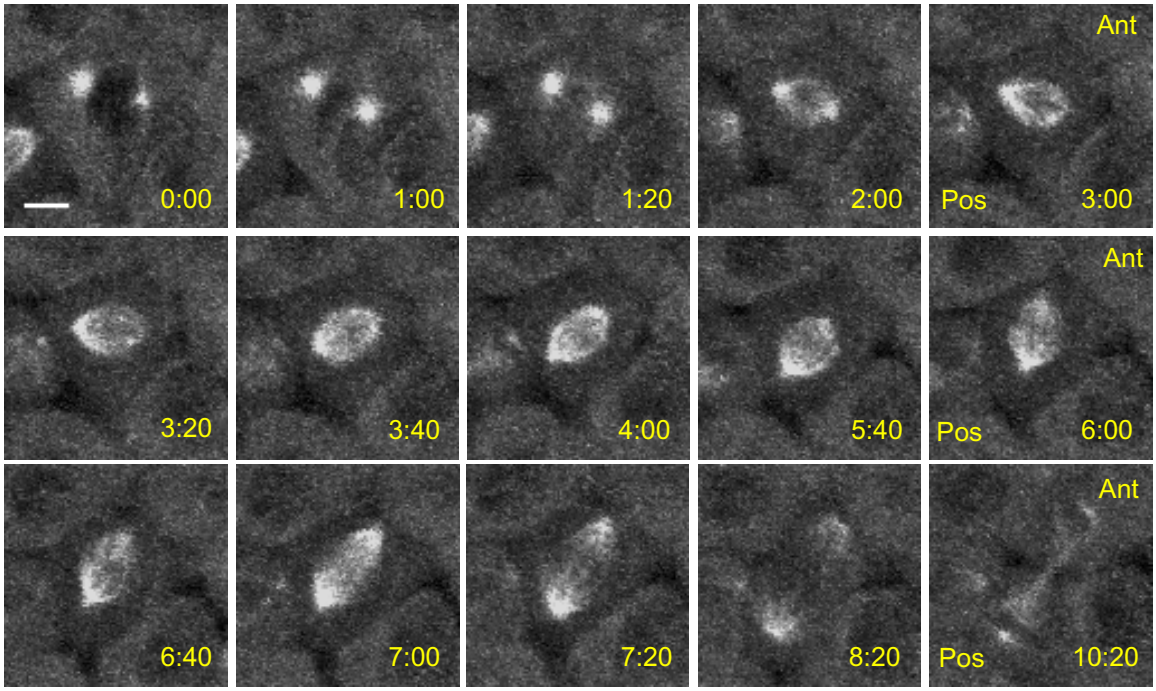

Figure 3-3 Spindle also reorients along the radial direction in the dorsal epiblast

Microtubules are revealed by α-tubulin-GFP in a wild-type gastrula. The anterior-posterior axis is along the diagonal of the images with anterior to the upper right. The XY images and reconstructed YZ images are show. The yellow line marks the position of the YZ images. The mitotic spindle forms in the YZ plane away from the anterior-posterior axis (t=0.00). The cross section of the spindle is visible in the XY plane. By t= 2:40, the spindle has to rotated to into the XY plane. It continues to rotate in the XY plane to align with the anterior-posterior axis (t=3:00 and t=3:20). Time is in minutes. Scale bar=6 μm.

Figure 3-3 Spindle also reorient along the radial direction in the dorsal epiblast

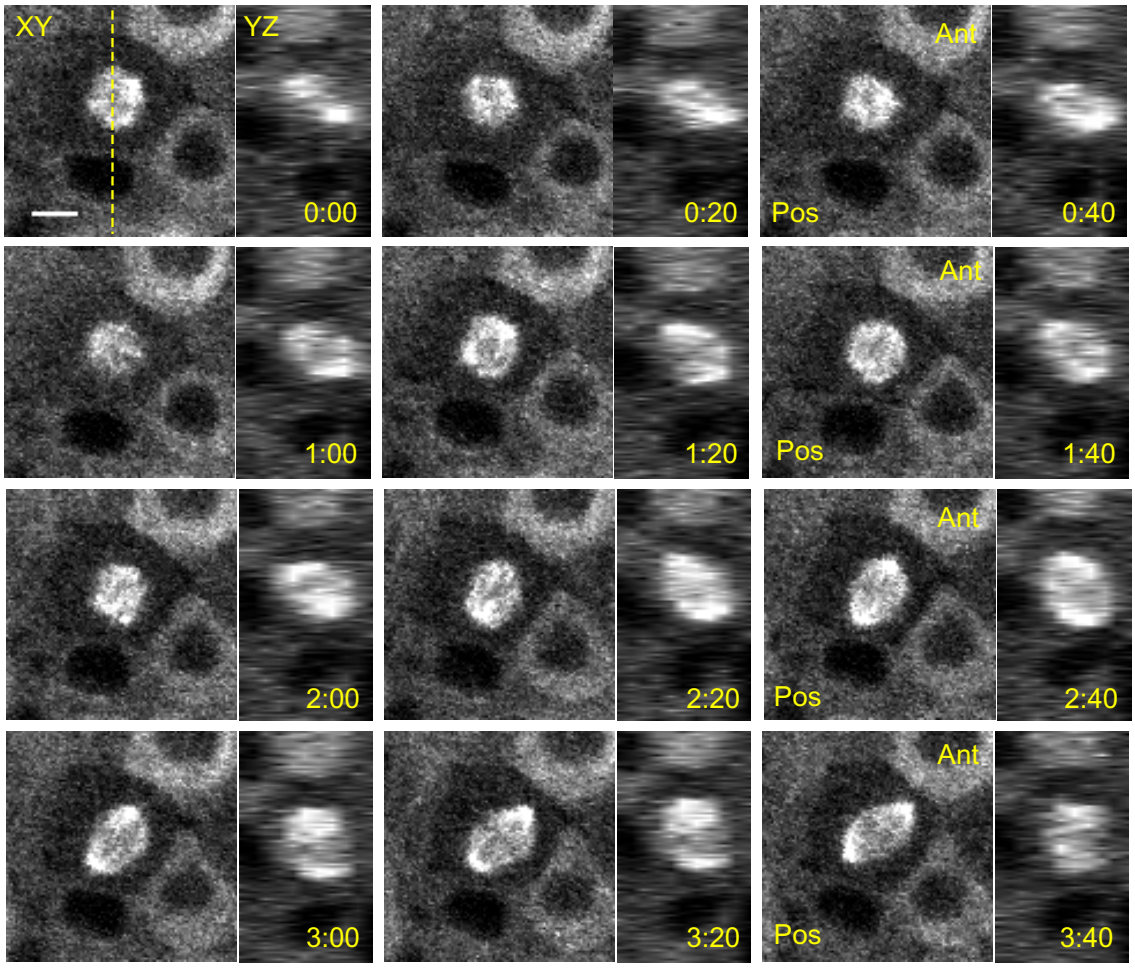

Figure 3-4 Spindle rotates away from the anterior-posterior axis in an Xdd1-overexpressing cell

Microtubules are revealed by α-tubulin-GFP in the dorsal epiblast. The anterior-posterior axis is along the diagonal of the images with anterior to the upper right. The spindle forms along the anterior-posterior axis (t=4:00 to 4:40). Then it rotates counter clockwise (t=5:00 to t=7:20). At anaphase, the two poles separate perpendicularly to the anterior-posterior axis (t=8:00 onwards). Time is in minutes. Scale bar=6 μm.

Figure 3-4 Spindle rotates away from the anterior-posterior axis in an Xdd1-overexpressing cell

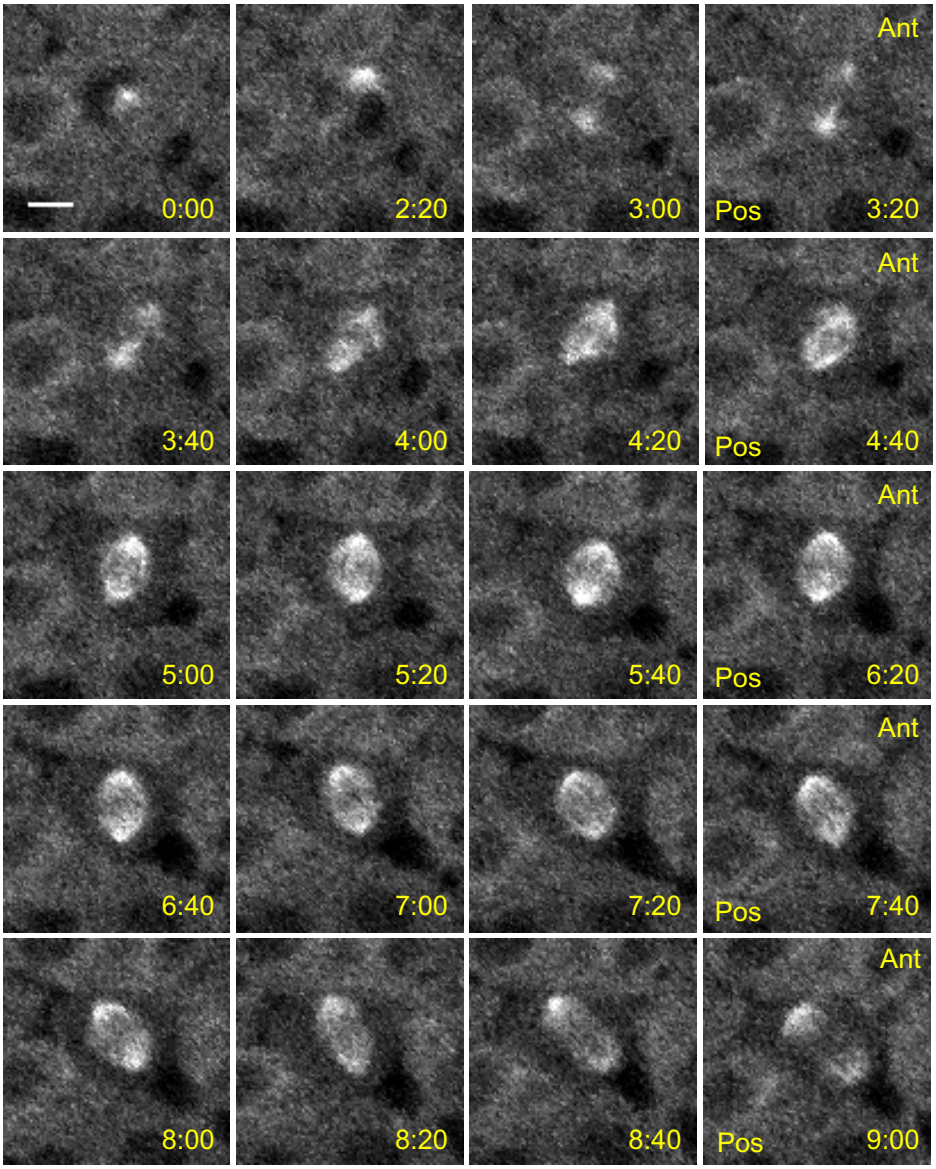

Figure 3-5 Spindle dynamics in another Xdd1 overexpressing cell

Microtubules are revealed by α-tubulin-GFP in the dorsal epiblast. The anterior-posterior axis is along the diagonal of the images with anterior to the upper right. Unlike the one in Figure 4, the spindle is formed at a 45^{o} angle to the anterior-posterior axis (t=2:00). If the spindle rotates counter clockwise for 45^{o}, it will align with the anterior-posterior axis. Instead, it rotates clockwise, away from the axis. At anaphase, the spindle poles separate at a near 90^{o} angle to the anterior-posterior axis (t=5:40). Time is in minutes. Scale bar=6 μm.

Figure 3-5 Spindle dynamics in another Xdd1-overexpressing cell

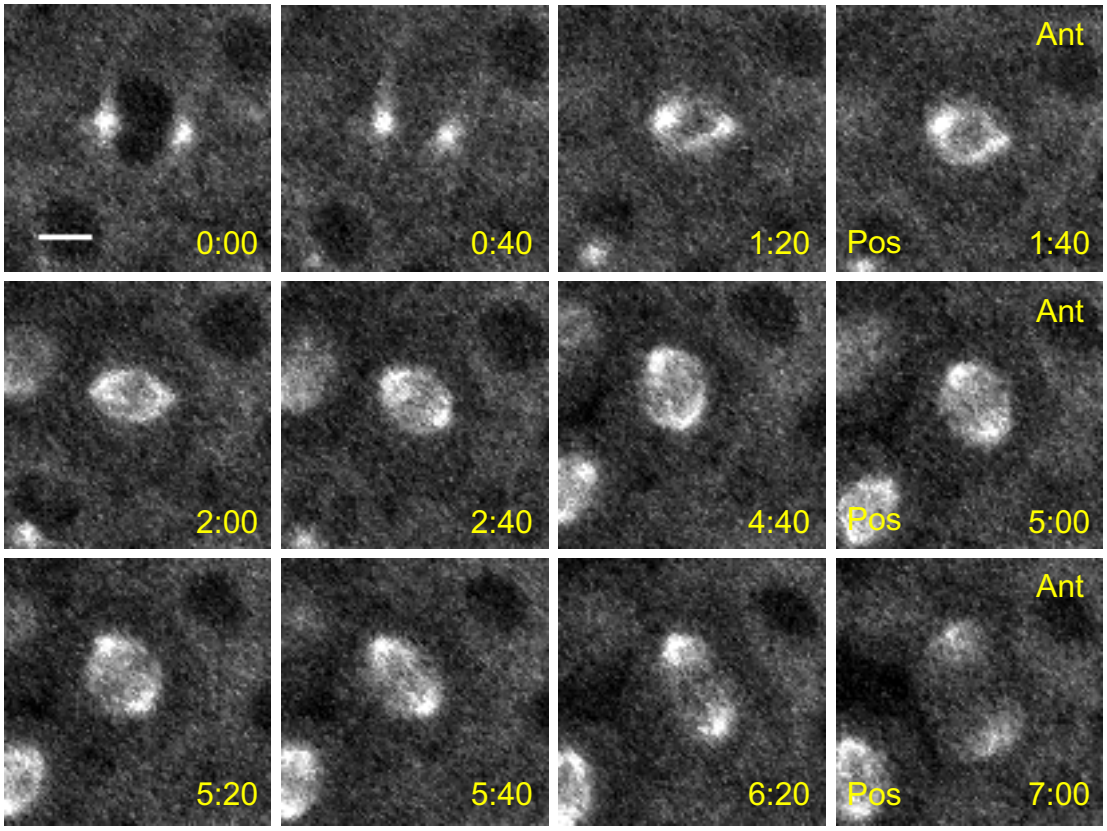

Chapter 4

Concluding remarks

In this thesis, I investigate the pattern, function, and regulation of mitotic divisions in zebrafish gastrulation. Using in vivo confocal imaging and quantitative analysis, I find that cells in dorsal axial tissues preferentially divide along the direction of tissue elongation, i.e., the anterior-posterior axis of the embryo. Establishment of the spindle polarity requires Silberblick/Wnt11, Dishevelled and Strabismus acting via the non-canonical Wnt/planar cell polarity (Wnt/PCP) pathway. On the subcellular level, oriented cell division is mediated by spindle rotation. The mitotic spindle forms at a random orientation and rotates at metaphase to line up with the anterior-posterior axis. Wnt/PCP signalling is not required for the spindle to rotate but dictates its destination. These data, together with previous work by others, demonstrate that cell polarization underlies the morphogenetic machinery that shapes the head-to-tail axis. In addition, Wnt/PCP signalling is involved in polarizing the cells, whose responses include medial-lateral elongation of the cell body and localization of protrusions, and anterior-posterior positioning of the mitotic spindle. These two types of polarized cell behaviours cooperate to shape the anterior-posterior body axis of the embryo. This work also demonstrates that the Wnt/PCP pathway is evolutionarily conserved as a strategy for cell polarization.

Contribution of this thesis

My thesis research's contribution to the field of developmental biology is two-fold. The first contribution lies in the findings that oriented division during

vertebrate axis elongation is under the control of the PCP pathway. Oriented cell division has long been proposed to play a role in axis elongation in vertebrates, but it is not known how this process is regulated. In my thesis, I have started to elucidate the molecular pathways controlling cell division orientation. My research's second contribution lies in the methodology. I have developed a quantitative method to analyze and present data concerning behaviours of large populations of cells. This method can, in principal, be applied to studies of other biological systems.

Oriented division and axis elongation

In my thesis, I have assessed how much anterior-posteriorly oriented cell division can contribute to axis elongation. An unanswered question is whether anterior-posteriorly oriented cell division is required for axis elongation. This is a necessity test, which requires specific disruption of division alignment. This may be achieved by targeting factors affecting orientation of the mitotic spindle. Dynein and dynactin are potential targets (Ahringer, 2003), though disruption of other cellular processes that involve dynein and dynactin could complicate interpretation of the results (Helfand et al., 2003). Nonetheless, I have obtained mutant constructs of dynein (Vaughan et al., 2001) and RNA overexpression experiments can be carried out rather easily.

Polarity and protein localization

Oriented division in zebrafish gastrulation is mediated by rotation of the mitotic spindle. The spindle sets up at a random orientation, and then rotates to line up with the anterior-posterior axis. When the PCP pathway is disrupted at the level of Dishevelled, the spindle still has the ability to rotate. But instead of rotating to line up with the anterior-posterior axis, the spindle rotates to a random end position. These results suggest that Dsh may participate in setting up the polarity cue that directs rotation of the spindle (see below).

Oriented cell division involves three steps of regulation: 1) receiving polarizing signal, 2) establishing polarity within the cell by forming polarity complexes, and 3) relaying polarity information to downstream cellular machinery that aligns the mitotic spindle. Multiple lines of evidence suggest that Dsh may be part of the cellular polarity complex. First, my finding that Dsh is not required for the spindle rotation per se, but dictates the end position of spindle rotation, suggests that Dsh is not part of the downstream machinery but instead is involved in setting up the polarity. Second, in *Drosophila*, Dsh is required for planar cell polarity in multiple contexts, including the wing, eye and sensory organ precursors (SOPs) (McNeill, 2002; Strutt, 2003). Dsh is part of a core polarity complex that is asymmetrically localized within the cells of the wing and eye (Axelrod, 2001; Shimada et al., 2001; Strutt et al., 2002). Although the subcellular localization of Dsh has not been directly looked at in the SOPs, Frizzled has been shown to asymmetrically localize in this case (Bellaiche et al., 2004; Bellaiche et al., 2001b). Moreover, there is also evidence that Dsh shows

subcellular localization in vertebrates. In *Xenopus* dorsal mesoderm explants undergoing convergent extension, ectopically expressed Dsh-GFP can be observed to accumulate at the medial-lateral ends of elongated cells (Kinoshita et al., 2003).

To gain insight to the function of Dsh, high-resolution subcellular localization data is necessary. The right experiment is to detect the endogenous Dsh using an antibody. There are antibodies to fly Dsh (Yanagawa et al., 1995) and human Dsh (Chemicon), but whether these reagents can cross-react with zebrafish Dsh in whole embryos needs to be determined. If these reagents do not work, low-level overexpression of Dsh-GFP can be used to provide some insight. We need to keep in mind that the localization pattern of ectopic protein may not reflect that of the endogenous one. A recent study of Kar9 localization in the budding yeast has illustrated this point very well (Liakopoulos et al., 2003)

Where is Dsh localized? It could also be localized to the medial-lateral ends of the cell while the spindle lines up with the anterior-posterior orientation. If this were the case, Dsh (and other members of the polarity complex) would work in a different way than in other systems such as *C. elegans* and *Drosophila* where the spindle lines up with the polarity complex. Dsh would “repel” instead of “attract” spindle poles. Whether Dsh localize to the medial-lateral cortex to repel or the anterior-posterior cortex to attract spindle, a persistent localization throughout interphase and mitosis may not be true. As discussed below, the polarity axis guiding spindle orientation appear to be established during mitosis. Alternatively, Dsh could accumulate at the medial-lateral ends during interphase

and at the anterior-posterior ends during mitosis. During interphase, it is responsible for cell elongation and generation of protrusions along the medial-lateral direction, while during mitosis, it directs mitotic spindle rotation. This is a wild speculation since it is not intuitive to conjure up a way that could lead to the switching of the polarity axis in our system. Cell division is not synchronous during zebrafish gastrulation, and thus those at interphase and those undergoing mitosis are intermixed with each other. In other words, mitotic and interphase cells are not spatially and temporally separable, which makes polarity switching an unlikely mechanism. Dsh could also localize uniformly around the cortex and acts as an adaptor for the “real” polarity proteins.

Appendix

Detailed Methods for Division Data Acquisition and Analysis

Data Acquisition

4D image sets are acquired using Zeiss 510 or Pascal. These images are stored as .lsm format with scaling parameters and other information included. The orientation of the embryo used for each imaging session is known and can be mapped onto the images. For each mitotic division, the (x,y,z,t) coordinates of both daughter nuclei during anaphase are obtained using the "ortho" function of the Zeiss LSM software (Fig. 1), and entered into an Excel spread sheet (Fig. 2). One Excel file is created for each embryo. In each Excel file, data is organized in 2 by 2 matrix. Each row contains data for one division. Column 1: an unique ID for each division; 2-4: x, y, z coordinates of the first daughter nucleus; 5-7: x ,y, z coordinates of the second daughter nucleus; 8: time point when division occurs; 9: which layer the cell is in--0 is for epiblast or surface; 1 is for hypoblast or deep. If this column is omitted, the processing scripts assume it is 0 and thus epiblast.

A parameter file is also created for each embryo (Fig. 3). 15 parameters are organized in one column. Parameters 1-3: x, y, z voxel dimension in microns; 4: t in seconds; 5-6: x low limit and x high limit (in pixels); 7-8: y low, y high; 9-10: z low, z high; 11-12: t low, t high; 13: needs stitching? (1 for yes, 0 for no. If there are more than one time lapse data from the same embryo, they can be concatenated); 14: length of time between the start of the first time lapse and that of the second time lapse, in seconds; 15: number shift added to the IC of the second time lapse (if it is 1000, the id of the second time lapse will start at 1001).

Both the data file and parameter file are exported as .txt. The

corresponding data and parameter files have the same name base, with the data file named “namebase.txt” and the parameter file named “namebase-para.txt”.

MATLAB scripts functionalities and syntax

autoscrn.m

Screens data, highlights and removes duplicates, unrealistically long (due to typing error when entering daughter nuclei coordinates), out-of-bound (according to parameters 1 to 12 in the parameter file) divisions.

Syntax: autoscrn('xdd1mos3-15-04')

Input files

- xdd1mos3-15-04.txt. Contains division data
- xdd1mos3-15-04-para.txt. Contains parameters

Output:

- atcor-xdd1mos3-15-04.txt. Will be used by processdiv3d.m.
- dump-xdd1mos2-21-04.txt
- autocor_bf.eps
- autocor_aft.eps

combine.m

Concatenates files for the same embryo.

Syntax: combine(‘atcor-stbm3-28-03-1.txt’,’actor-stbm3-28-03-2.txt’,

‘atcor-stbm3-28-03.txt’)

Input files

- atcor-stbm3-28-03-1.txt. Corrected data file.
- atcor-stbm3-28-03-2.txt. Corrected data file.

Output file:

- atcor-stbm3-28-03.txt

processdiv3d.m

Processes the corrected division data. Uses two methods to process 3 dimensional data. Method1 breaks down each division into its planar components (XY, YZ, XZ respectively). It calculates each planar component's angle with respect to the animal-vegetal axis (AV). Method 2 uses what is conventionally used for an epithelium. It calculates the angle in 3D with respect to the AV, and the angle with the XY plane (the epiblast plane—analogous to the epithelial plane). Results obtained using the first method are presented in this thesis.

Syntax**:** processdiv3d('xdd1mos3-15-04')

Input file

- actor-xdd1mos3-15-04.txt

Output files

- xdd1mos3-15-04.agl
- xdd1mos3-15-04.sts
- xdd1mos3-15-04, which will be used by divstats.m.
- divfig1.eps. Graphic representation in three planes, each division is normalized to the same length. Also has total x, total y, total z in 30 min time windows.
- divfig2.eps: histograms of division angles and cumulative plots of

division angles.

Divstats.m

Takes data from all animals under one experimental condition and performs statistical analysis.

Syntax: divstats('xdd1mos')

Input files:

- xdd1mos.txt. Contains names of data files to be included in the analysis.
- MATLAB data files generated for each animal by processdiv3d.

Output file:

- xdd1mos.eps. Plots the cumulative distribution of division angles by the two different methods employed by processdiv3d.m. Lists all statistics.

Source codes for MATLAB scripts

autoscrn.m

```
function autoscrn(filenamebase);

datafile=sprintf('%s.txt',filenamebase);
prafile=sprintf('%s-para.txt',filenamebase);
outputfile1='autocor_bf.eps';
outputfile2='autocor_aft.eps';
outputfile3=sprintf('dump-%s',datafile);
outputfile4=sprintf('atcor-%s',datafile);
data=load(datafile);
pradata=load(prafile)
totalcellno=size(data,1);

%screen for wrong coordinates that result in long lines
```

```
distcutoff=50;
midcutoff=10;
dims=4;
%dims has to be 2-4.

%%%%read the following parameters from parameter file
xscale=pradata(1); %pixel size in um
yscale=pradata(2); %pixel size in um
zscale=pradata(3); %z depth in um
tscale=pradata(4); %second
xlimlow=pradata(5).*xscale; %x keep range before correction
xlimhigh=pradata(6).*xscale; %x keep range before correction
ylimlow=pradata(7).*yscale; %x keep range before correction
ylimhigh=pradata(8).*yscale; %x keep range before correction
zlimlow=pradata(9).*zscale; %x keep range before correction
zlimhigh=pradata(10).*zscale; %x keep range before correction
tlimlow=pradata(11).*tscale/60.0; %x keep range before correction
tlimhigh=pradata(12).*tscale/60.0; %x keep range before
correction


data(:,2)=data(:,2)*xscale;
data(:,3)=data(:,3)*yscale;
data(:,4)=data(:,4)*zscale;
data(:,5)=data(:,5)*xscale;
data(:,6)=data(:,6)*yscale;
data(:,7)=data(:,7)*zscale;
data(:,8)=data(:,8)*tscale/60.0;


dist=sqrt((data(:,2)-data(:,5)).^2+(data(:,3)-
data(:,6)).^2+(data(:,4)-data(:,7)).^2);


maxX=max([max(data(:,2)) max(data(:,5))]);
minX=min([min(data(:,2)) min(data(:,5))]);
maxY=max([max(data(:,3)) max(data(:,6))]);
minY=min([min(data(:,3)) min(data(:,6))]);

figure(1);
clf;
plottitle=sprintf('%s******%ddivisions',filenamebase,totalcellno)
;
title(plottitle);
xlabel('Mediolateral');
ylabel('A-P');
hold on;
for i=1:size(data,1)

   h=plot([data(i,2) data(i,5)],[data(i,3) data(i,6)]);
   set(h,'linewidth',[1]);
end

%%%%screen for wrong coordinates
number_wrong=0;
tmp_idx=dist>distcutoff;
tmp_data=data(tmp_idx,:);
number_wrong=number_wrong+size(tmp_data,1);
```

```
wrongkeep=[];
for i=1:size(tmp_data,1)
    wrongkeep=[wrongkeep; tmp_data(i,1)];
   h=plot([tmp_data(i,2) tmp_data(i,5)],[tmp_data(i,3)
tmp_data(i,6)],'c');
   set(h,'linewidth',[1]);
   h=text(tmp_data(i,2),tmp_data(i,3), num2str(tmp_data(i,1)));
   set(h,'color','c');
end
tmp_data=data(~tmp_idx,:);
data=tmp_data;

%exclude out of range data
tmp_idx=(data(:,2)<xlimlow | data(:,2)>xlimhigh |
data(:,5)<xlimlow | data(:,5)>xlimhigh |data(:,3)<ylimlow |
data(:,3)>ylimhigh | data(:,6)<ylimlow | data(:,6)>ylimhigh
|data(:,4)<zlimlow | data(:,4)>zlimhigh | data(:,7)<zlimlow |
data(:,7)>zlimhigh |data(:,8)<tlimlow | data(:,8)>tlimhigh);
tmp_data=data(tmp_idx,:);
number_wrong=number_wrong+size(tmp_data,1);

for i=1:size(tmp_data,1)
    wrongkeep=[wrongkeep; tmp_data(i,1)];
   h=plot([tmp_data(i,2) tmp_data(i,5)],[tmp_data(i,3)
tmp_data(i,6)],'g');
   set(h,'linewidth',[1]);
   h=text(tmp_data(i,2),tmp_data(i,3), num2str(tmp_data(i,1)));
   set(h,'color','g');
end
tmp_data=data(~tmp_idx,:);
data=tmp_data;

%%%%%%%%screen for duplicaton
mid=[(data(:,2)+data(:,5))/2 (data(:,3)+data(:,6))/2
(data(:,4)+data(:,7))/2];

for i=1:size(data,1)-1
    for j=i+1:size(data,1)
        if (dims==2)
           mid_dist=sqrt((mid(i,1)-mid(j,1))^2+(mid(i,2)-
mid(j,2))^2);
        end

        if (dims==3)
           mid_dist=sqrt((mid(i,1)-mid(j,1))^2+(mid(i,2)-
mid(j,2))^2+(mid(i,3)-mid(j,3))^2);
        end

        if (dims==4)
            mid_dist=sqrt((mid(i,1)-mid(j,1))^2+(mid(i,2)-
mid(j,2))^2+(mid(i,3)-mid(j,3))^2 +(data(i,8)-data(j,8))^2);
        end
        if (mid_dist<midcutoff)
             wrongkeep=[wrongkeep;data(j,1)];
             h=plot([data(i,2) data(i,5)],[data(i,3)
data(i,6)],'r');
             h=plot([data(j,2) data(j,5)],[data(j,3)
data(j,6)],'r');
```

```
            h=text(data(i,2),data(i,3), num2str([data(i,1)
data(j,1)]));
            set(h,'color','r');


        end
    end
end


axis([minX maxX minY maxY]);
set(gca,'DataAspectRatio',[1 1 1]);
set(gca,'Ydir','reverse');

print('-depsc',outputfile1);
save(outputfile3,'wrongkeep','-ascii');

figure(2);
clf;
datakeep=[];
for i=1:size(data,1)
    if (any(wrongkeep==data(i,1)))

    else
        datakeep=[datakeep;data(i,:)];
    end
end
keepcellno=totalcellno-size(wrongkeep,1);
plottitle=sprintf('%s******%ddivisions',filenamebase,keepcellno);

title(plottitle);
xlabel('Mediolateral');
ylabel('A-P');
hold on;
for i=1:size(datakeep,1)

   h=plot([datakeep(i,2) datakeep(i,5)],[datakeep(i,3)
datakeep(i,6)]);
   set(h,'linewidth',[1]);
end

axis([minX maxX minY maxY]);
set(gca,'DataAspectRatio',[1 1 1]);
set(gca,'Ydir','reverse');
print('-depsc',outputfile2);

if (pradata(13)==1)
         datakeep(:,8)=datakeep(:,8)+pradata(14)/60;
         datakeep(:,1)=datakeep(:,1)+pradata(15);

end

save(outputfile4,'datakeep','-ascii');
```

combine.m

```
function combine(f1,f2,f3);

a=load(f1);
b=load(f2);
c=[a;b];
save(f3,'c','-ascii');
```

processdiv3d.m

```
function processdiv3d(filenamebase);

datafile=sprintf('%s.txt',filenamebase);
%prafile=sprintf('%s-para.txt',filenamebase);
corfile=sprintf('atcor-%s',datafile);

time_per_seg=30; %in minutes

%pradata=load(prafile);
dataall=load(corfile);
%tscale=pradata(4); %second

looptime=0;
if (size(dataall,2)>8)
    looptime=1;
end

for layer=0:looptime
    data=dataall;
    if (size(dataall,2)>8)
        idx=dataall(:,9)==layer;
        data=dataall(idx,:);
    end

%x range. percentage
xlow=0;
xhigh=1;
totaltime=max(data(:,8));

time_interval=ceil(totaltime/time_per_seg);
results=zeros(time_interval,5);

for i=1:time_interval
   tmp_idx=((data(:,8)>time_per_seg*(i-1))&
(data(:,8)<=time_per_seg*i));
   tmp_data=data(tmp_idx,:);
   dist=sqrt((tmp_data(:,2)-tmp_data(:,5)).^2+(tmp_data(:,3)-
tmp_data(:,6)).^2+(tmp_data(:,4)-tmp_data(:,7)).^2);
   results(i,1)=results(i,1)+sum(abs(tmp_data(:,2)-
tmp_data(:,5))./dist);
   results(i,2)=results(i,2)+sum(abs(tmp_data(:,3)-
tmp_data(:,6))./dist);
   results(i,3)=results(i,3)+sum(abs(tmp_data(:,4)-
tmp_data(:,7))./dist);
   results(i,4)=results(i,2)./results(i,1);
   results(i,5)=results(i,2)./results(i,3);
   results(i,6)=size(tmp_data,1);

end
disp='X   Y   Z   Y/X   Y/Z  CellNo';
results;

figure(2*layer+1);
clf;
```

```
subplot(2,2,3)
title('X-Y Plane');
xlabel('Mediolateral');
ylabel('A-P');
hold on;
for i=1:size(data,1)

   h=plot([data(i,2) data(i,5)],[data(i,3) data(i,6)]);
   set(h,'linewidth',[1]);
end
set(gca,'DataAspectRatio',[1 1 1]);
set(gca,'Ydir','reverse');


subplot(2,2,4)
title('Y-Z Plane');
xlabel('Z-Depth');
ylabel('A-P');
hold on;
for i=1:size(data,1)

   h=plot([data(i,4) data(i,7)],[data(i,3) data(i,6)]);
   set(h,'linewidth',[1]);
end
set(gca,'DataAspectRatio',[1 1 1]);
set(gca,'Ydir','reverse');
set(gca,'Xdir','reverse');


subplot(2,2,1)
title('Z-X Plane');
xlabel('Mediolateral');
ylabel('Z-depth');
hold on;
for i=1:size(data,1)

   h=plot([data(i,2) data(i,5)],[data(i,4) data(i,7)]);
   set(h,'linewidth',[1]);
end
set(gca,'DataAspectRatio',[1 1 1]);
set(gca,'Ydir','reverse');
%totalX
%totalY
%totalZ

subplot(2,2,2)
set(gca,'Visible','off');
if (layer==0)
   text(0.1,1,datafile);
   text(0.7,1,'surface');
end
if (layer==1)
   text(0.1,1,datafile);
   text(0.7,1,'deep');
end
```

```
printtmp=sprintf('%s\t\%s\t%s\t%s\t%s\t%s','M-L','A-P','Z
Depth','Y/X','Y/Z','CellNo');
text(0,0.7,'X       Y      Z    Y/X  Y/Z  DivNO');
printtmp=sprintf('TPS %d min',time_per_seg');
text(0.4,0.9,printtmp);
for i=1:time_interval
printtmp=sprintf('%4.1f  %4.1f  %4.1f  %4.1f  %4.1f
%d',results(i,1),results(i,2),results(i,3),results(i,4),results(i
,5),results(i,6));
text(0,0.6-(i-1)*0.1,printtmp);
end
figure(2*layer+2);
clf;

x=abs(data(:,2)-data(:,5));
y=abs(data(:,3)-data(:,6));
z=abs(data(:,4)-data(:,7));
angleYX=atan(x./(y+0.000001))/pi*180;
angleYZ=atan(z./(y+0.000001))/pi*180;
angleY=acos(y./sqrt(x.^2+y.^2+z.^2))/pi*180;
angleZ=acos(z./sqrt(x.^2+y.^2+z.^2))/pi*180;
angleZ=90-angleZ;

angles=[angleYX angleYZ angleY angleZ];

anglebin=0:10:80;
subplot(4,2,1);
nyx=hist(angleYX,anglebin);
nyx=nyx./size(data,1);
bar(anglebin+5,nyx);
axis([0 90 0 1.0]);
%xlabel('Planar angle with anterior-posterior axis [degrees]');
ylabel('Divisions (%)');
title(datafile);
set(gca,'box','off');
set(gca,'tickdir','out');
set(gca,'plotboxaspectratio',[1 1 1]);

subplot(4,2,2);
nyz=hist(angleYZ,anglebin);
nyz=nyz./size(data,1);
bar(anglebin+5,nyz);
axis([0 90 0 1.0]);
%xlabel('Radial angle with anterior-posterior axis [degrees]');
ylabel('Divisions (%)');
if (layer==0)
    title('surface');
else
    title('deep');
end

nyxc=zeros(size(anglebin,2),1);
nyzc=zeros(size(anglebin,2),1);
for i=1:size(anglebin,2)
   nyxc(i)=sum(nyx(1:i));
   nyzc(i)=sum(nyz(1:i));
end
set(gca,'box','off');
```

```
set(gca,'tickdir','out');
set(gca,'plotboxaspectratio',[1 1 1]);


subplot(4,2,3);
bar(anglebin+5,nyxc);
axis([0 90 0 1.0]);
xlabel('XY planar angle with anterior-posterior axis [degrees]');
ylabel('Cumulative (%)');
set(gca,'box','off');
set(gca,'tickdir','out');
set(gca,'plotboxaspectratio',[1 1 1]);


subplot(4,2,4);
bar(anglebin+5,nyzc);
axis([0 90 0 1.0]);
xlabel('YZ planar angle with anterior-posterior axis [degrees]');
ylabel('Cumulative (%)');
set(gca,'box','off');
set(gca,'tickdir','out');
set(gca,'plotboxaspectratio',[1 1 1]);

subplot(4,2,5);
ny=hist(angleY,anglebin);
ny=ny./size(data,1);
bar(anglebin+5,ny);
axis([0 90 0 1.0]);
%xlabel('3-D angle with anterior-posterior axis [degrees]');

ylabel('Divisions (%)');
%title(datafile);
set(gca,'box','off');
set(gca,'tickdir','out');
set(gca,'plotboxaspectratio',[1 1 1]);

subplot(4,2,6);
nz=hist(angleZ,anglebin);
nz=nz./size(data,1);
bar(anglebin+5,nz);
axis([0 90 0 1.0]);
%xlabel('3D angle with X-Y Plan [degrees]');
ylabel('Divisions (%)');

nyxc=zeros(size(anglebin,2),1);
nyzc=zeros(size(anglebin,2),1);

nyc=zeros(size(anglebin,2),1);
nzc=zeros(size(anglebin,2),1);

for i=1:size(anglebin,2)
   nyxc(i)=sum(nyx(1:i));
   nyzc(i)=sum(nyz(1:i));
   nyc(i)=sum(ny(1:i));
   nzc(i)=sum(nz(1:i));

end
set(gca,'box','off');
```

```
set(gca,'tickdir','out');
set(gca,'plotboxaspectratio',[1 1 1]);


subplot(4,2,7);
bar(anglebin+5,nyc);
axis([0 90 0 1.0]);
xlabel('3-D angle with anterior-posterior axis [degrees]');
ylabel('Cumulative (%)');
set(gca,'box','off');
set(gca,'tickdir','out');
set(gca,'plotboxaspectratio',[1 1 1]);


subplot(4,2,8);
bar(anglebin+5,nzc);
axis([0 90 0 1.0]);
xlabel('3-D angle with X-Y Plane [degrees]');
ylabel('Cumulative (%)');
set(gca,'box','off');
set(gca,'tickdir','out');
set(gca,'plotboxaspectratio',[1 1 1]);


nykeep=[nyx' nyxc nyz' nyzc ny' nyc nz' nzc];

if (layer==0)
    outfile1=sprintf('%s.res',filenamebase);
    outfile2=sprintf('%s.sts',filenamebase);
    outfile3=sprintf('%s.agl',filenamebase);
    outfile4=sprintf('%s.mat',filenamebase);
else
    outfile1=sprintf('deep-%s.res',filenamebase);
    outfile2=sprintf('deep-%s.sts',filenamebase);
    outfile3=sprintf('deep-%s.agl',filenamebase);
    outfile4=sprintf('deep-%s.mat',filenamebase);
end
num_div=size(angles,1);
angle45yx=sum(angles(:,1)<45)/num_div;
angle45yz=sum(angles(:,2)<45)/num_div;
angle45y=sum(angles(:,3)<45)/num_div;
angle45z=sum(angles(:,4)<45)/num_div;

yxproject=sum(results(:,2))/sum(results(:,1));
yzproject=sum(results(:,2))/sum(results(:,3));

anglekeep=[angle45yx angle45yz angle45y angle45z num_div];

save(outfile1,'results','-ascii');
save(outfile2,'nykeep','-ascii');
save(outfile3,'angles','-ascii');
save(outfile4,'results','nykeep','angles','anglekeep','anglebin')
;
end

figure(1);
print -depsc divfig1.eps;
figure(2);
```

```
print -depsc divfig2.eps;
if (size(dataall,2)>8)
figure(3);
print -depsc divfig3.eps;
figure(4);
print -depsc divfig4.eps;

end
```

divstats.m

```
function divstats(filenamebase);
datafilename=sprintf('%s.txt',filenamebase);
datafile=textread(datafilename,'%s');
num_animal=size(datafile,1);

for i=1:num_animal

    load(datafile{i});
    curvedata(:,:,i)=nykeep;
    bardata(:,i)=anglekeep';
end

meancurvedata=mean(curvedata,3);
stdcurvedata=std(curvedata,0,3);

meanbardata=mean(bardata,2);
stdbardata=std(bardata,0,2);
totaldiv=sum(bardata(5,:));

clf;

lw=3;
lw1=2;
subplot(3,2,1);
hold on;
h=plot(anglebin+10,meancurvedata(:,2)*100);
set(h,'linewidth',lw);
h=errorbar(anglebin+10,meancurvedata(:,2)*100,stdcurvedata(:,2)*1
00);
set(h,'linewidth',lw1);
axis([min(anglebin+10), max(anglebin+10), 0 100]);
xlabel('YX planar angle with AP [degree]');
ylabel('Cumulative percentage');

subplot(3,2,2);
hold on;
h=plot(anglebin+10,meancurvedata(:,4)*100);
set(h,'linewidth',lw);
h=errorbar(anglebin+10,meancurvedata(:,4)*100,stdcurvedata(:,4)*1
00);
set(h,'linewidth',lw1);
axis([min(anglebin+10), max(anglebin+10), 0 100]);
xlabel(' YZ planar angle with AP[degree]');
ylabel('Cumulative percentage');

subplot(3,2,3);
hold on;
h=plot(anglebin+10,meancurvedata(:,6)*100);
set(h,'linewidth',lw);
h=errorbar(anglebin+10,meancurvedata(:,6)*100,stdcurvedata(:,6)*1
00);
set(h,'linewidth',lw1);
axis([min(anglebin+10), max(anglebin+10), 0 100]);
xlabel('3D angle with AP [degree]');
ylabel('Cumulative percentage');
```

```
subplot(3,2,4);
hold on;
h=plot(anglebin+10,meancurvedata(:,8)*100);
set(h,'linewidth',lw);
h=errorbar(anglebin+10,meancurvedata(:,8)*100,stdcurvedata(:,8)*1
00);
set(h,'linewidth',lw1);
axis([min(anglebin+10), max(anglebin+10), 0 100]);
xlabel('3D angle with X-Y plane[degree]');
ylabel('Cumulative percentage');

subplot(3,2,5);
%hold on;
%h=bar(meanbardata(1:4));
set(gca,'Visible','off');
text(0.3,1.0,filenamebase);

strtmp=sprintf('YX within 45 degree:%4.3f+/-
%4.3f',meanbardata(1),stdbardata(1));
text(0,0.8,strtmp);
strtmp=sprintf('YZ within 45 degree:%4.3f+/-
%4.3f',meanbardata(2),stdbardata(2));
text(0,0.6,strtmp);
strtmp=sprintf('3D Y within 45 degree:%4.3f+/-
%4.3f',meanbardata(3),stdbardata(3));
text(0,0.4,strtmp);
strtmp=sprintf('3D Y-X within 45 degree:%4.3f+/-
%4.3f',meanbardata(4),stdbardata(4));
text(0,0.2,strtmp);
strtmp=sprintf('Total %d divisions from %d animals',
totaldiv,num_animal);
text(0,0.0,strtmp);

subplot(3,2,6);
set(gca,'Visible','off');
 text(0.3,1,'Data Sets');
for i=1:num_animal
    text(0,1-i*0.2,datafile{i});
end

outfile1=sprintf('%s.mat',filenamebase);
save(outfile1,'meancurvedata','stdcurvedata','meanbardata','stdba
rdata','totaldiv','num_animal');
outfile2=sprintf('%s.eps',filenamebase);
print('-depsc',outfile2);
```

Figure 4-1 Method for acquiring division data

Time-lapse images are visualized using the Zeiss LSM software. For each mitotic division, the (x,y,z,t) coordinates of both daughter nuclei during anaphase are obtained using the “ortho” function of the Zeiss LSM software.

Figure 4-1 Method for acquiring division data

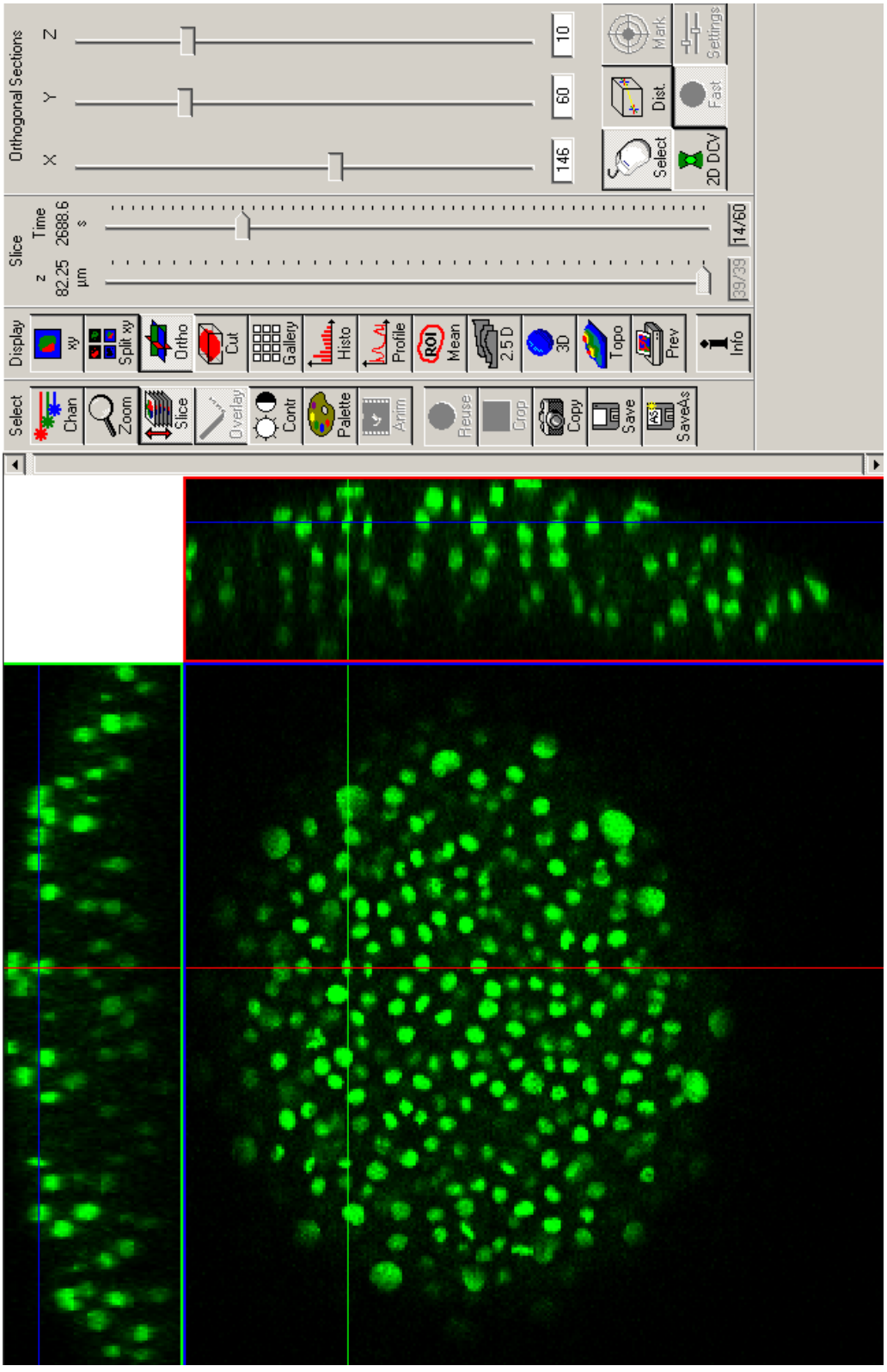

Figure 4-2 Division data structure

Data is organized in a 2 by 2 matrix. Each row contains data for one division. Id: an unique ID for each division; x1, y1, z1: x, y, z coordinates of the first daughter nucleus; x2, y2, z2: x ,y, z coordinates of the second daughter nucleus; t: time point when division occurs; hypoblast: which layer the cell is in--0 is for epiblast or surface; 1 is for hypoblast or deep. If this column is omitted, the processing scripts assume it is 0 and thus epiblast.

Figure 4-2 Division data structure

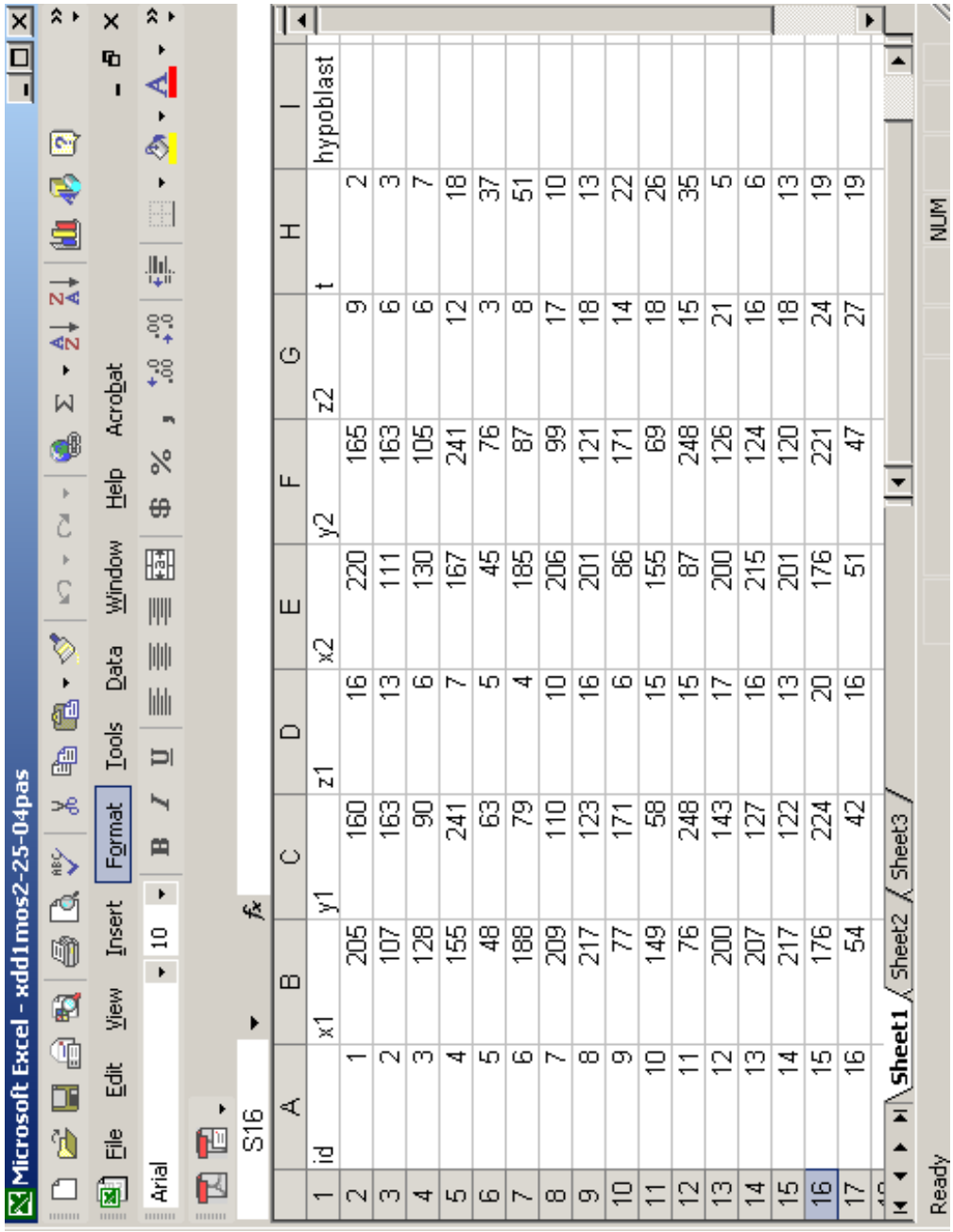

	A	B	C	D	E	F	G	H	I
1	id	x1	y1	z1	x2	y2	z2	t	hypoblast
2	1	205	160	16	220	165	9	2	
3	2	107	163	13	111	163	6	3	
4	3	128	90	6	130	105	6	7	
5	4	155	241	7	167	241	12	18	
6	5	48	63	5	45	76	3	37	
7	6	188	79	4	185	87	8	51	
8	7	209	110	10	206	99	17	10	
9	8	217	123	16	201	121	18	13	
10	9	77	171	6	86	171	14	22	
11	10	149	58	15	155	69	18	26	
12	11	76	248	15	87	248	15	35	
13	12	200	143	17	200	126	21	5	
14	13	207	127	16	215	124	16	6	
15	14	217	122	13	201	120	18	13	
16	15	176	224	20	176	221	24	19	
17	16	54	42	16	51	47	27	19	

Figure 4-3 Parameter file organization

15 parameters are organized in one column. Parameters 1-3: x, y, z voxel dimension in microns; 4: t in seconds; 5-6: x low limit and x high limit (in pixels); 7-8: y low, y high; 9-10: z low, z high; 11-12: t low, t high; 13: needs stitching? (1 for yes, 0 for no. If there are more than one time lapse data from the same embryo, they can be concatenated); 14: length of time between the start of the first time lapse and that of the second time lapse, in seconds; 15: number shift added to the IC of the second time lapse (if it is 1000, the id of the second time lapse will start at 1001).

Figure 4-3 Parameter file organization

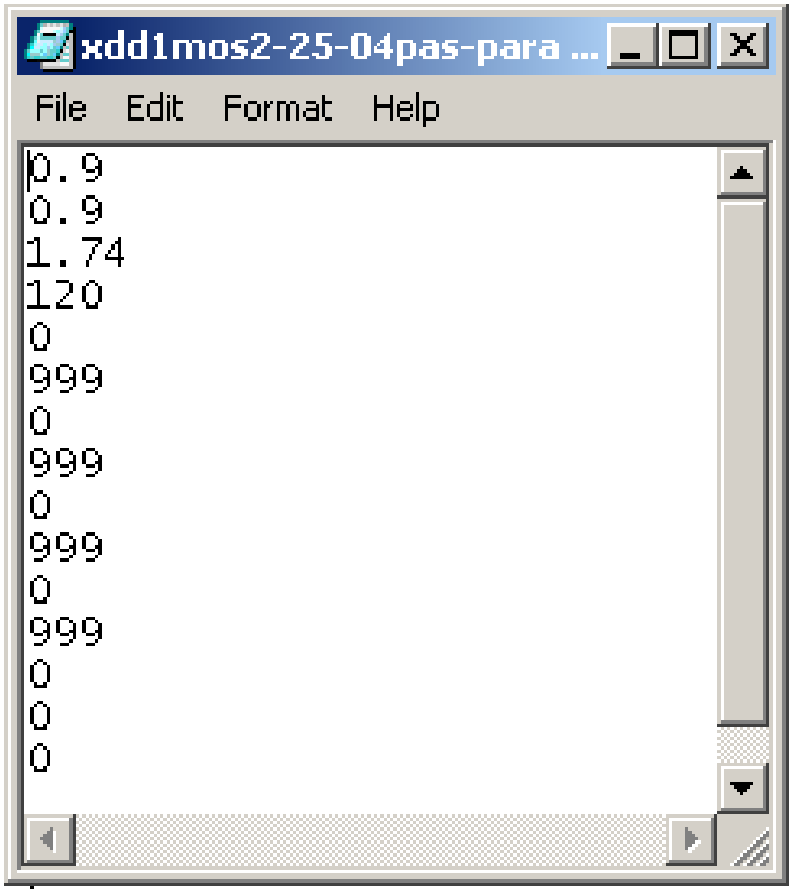

Bibliography

Ahringer, J. (2003). Control of cell polarity and mitotic spindle positioning in animal cells. *Curr Opin Cell Biol* **15**, 73-81.

Axelrod, J. D. (2001). Unipolar membrane association of Dishevelled mediates Frizzled planar cell polarity signaling. *Genes Dev* **15**, 1182-7.

Axelrod, J. D., Miller, J. R., Shulman, J. M., Moon, R. T. and Perrimon, N. (1998). Differential recruitment of Dishevelled provides signaling specificity in the planar cell polarity and Wingless signaling pathways. *Genes Dev* **12**, 2610-22.

Bardin, A. J., Le Borgne, R. and Schweisguth, F. (2004). Asymmetric localization and function of cell-fate determinants: a fly's view. *Curr Opin Neurobiol* **14**, 6-14.

Bellaiche, Y., Beaudoin-Massiani, O., Stuttem, I. and Schweisguth, F. (2004). The planar cell polarity protein Strabismus promotes Pins anterior localization during asymmetric division of sensory organ precursor cells in Drosophila. *Development* **131**, 469-78.

Bellaiche, Y., Gho, M., Kaltschmidt, J. A., Brand, A. H. and Schweisguth, F. (2001a). Frizzled regulates localization of cell-fate determinants and mitotic spindle rotation during asymmetric cell division. *Nat Cell Biol* **3**, 50-7.

Bellaiche, Y., Radovic, A., Woods, D. F., Hough, C. D., Parmentier, M. L., O'Kane, C. J., Bryant, P. J. and Schweisguth, F. (2001b). The Partner of Inscuteable/Discs-large complex is required to establish planar polarity during asymmetric cell division in Drosophila. *Cell* **106**, 355-66.

Cadigan, K. M. and Nusse, R. (1997). Wnt signaling: a common theme in animal development. *Genes Dev* **11**, 3286-305.

Carreira-Barbosa, F., Concha, M. L., Takeuchi, M., Ueno, N., Wilson, S. W. and Tada, M. (2003). Prickle 1 regulates cell movements during gastrulation and neuronal migration in zebrafish. *Development* **130**, 4037-46.

Chia, W. and Yang, X. (2002). Asymmetric division of Drosophila neural progenitors. *Curr Opin Genet Dev* **12**, 459-64.

Concha, M. L. and Adams, R. J. (1998). Oriented cell divisions and cellular morphogenesis in the zebrafish gastrula and neurula: a time-lapse analysis. *Development* **125**, 983-94.

Curtin, J. A., Quint, E., Tsipouri, V., Arkell, R. M., Cattanach, B., Copp, A. J., Henderson, D. J., Spurr, N., Stanier, P., Fisher, E. M. et al. (2003). Mutation of Celsr1 disrupts planar polarity of inner ear hair cells and causes severe neural tube defects in the mouse. *Curr Biol* **13**, 1129-33.

Darken, R. S., Scola, A. M., Rakeman, A. S., Das, G., Mlodzik, M. and Wilson, P. A. (2002). The planar polarity gene strabismus regulates convergent extension movements in Xenopus. *Embo J* **21**, 976-85.

Davidson, L. A., Hoffstrom, B. G., Keller, R. and DeSimone, D. W. (2002). Mesendoderm extension and mantle closure in Xenopus laevis gastrulation: combined roles for integrin alpha(5)beta(1), fibronectin, and tissue geometry. *Dev Biol* **242**, 109-29.

Djiane, A., Riou, J., Umbhauer, M., Boucaut, J. and Shi, D. (2000). Role of frizzled 7 in the regulation of convergent extension movements during gastrulation in Xenopus laevis. *Development* **127**, 3091-100.

Du, S. J., Purcell, S. M., Christian, J. L., McGrew, L. L. and Moon, R. T. (1995). Identification of distinct classes and functional domains of Wnts through expression of wild-type and chimeric proteins in Xenopus embryos. *Mol Cell Biol* **15**, 2625-34.

Elul, T. and Keller, R. (2000). Monopolar protrusive activity: a new morphogenic cell behavior in the neural plate dependent on vertical interactions with the mesoderm in Xenopus. *Dev Biol* **224**, 3-19.

Elul, T., Koehl, M. A. and Keller, R. (1997). Cellular mechanism underlying neural convergent extension in Xenopus laevis embryos. *Dev Biol* **191**, 243-58.

Etienne-Manneville, S. and Hall, A. (2002). Rho GTPases in cell biology. *Nature* **420**, 629-35.

Ezin, A. M., Skoglund, P. and Keller, R. (2003). The midline (notochord and notoplate) patterns the cell motility underlying convergence and extension of the Xenopus neural plate. *Dev Biol* **256**, 100-14.

Gho, M. and Schweisguth, F. (1998). Frizzled signalling controls orientation of asymmetric sense organ precursor cell divisions in Drosophila. *Nature* **393**, 178-81.

Gilland, E., Miller, A. L., Karplus, E., Baker, R. and Webb, S. E. (1999). Imaging of multicellular large-scale rhythmic calcium waves during zebrafish gastrulation. *Proc Natl Acad Sci U S A* **96**, 157-61.

Glickman, N. S., Kimmel, C. B., Jones, M. A. and Adams, R. J. (2003). Shaping the zebrafish notochord. *Development* **130**, 873-87.

Gonczy, P. (2002). Mechanisms of spindle positioning: focus on flies and worms. *Trends Cell Biol* **12**, 332-9.

Goto, T. and Keller, R. (2002). The planar cell polarity gene strabismus regulates convergence and extension and neural fold closure in Xenopus. *Dev Biol* **247**, 165-81.

Gundersen, G. G. and Bretscher, A. (2003). Cell biology. Microtubule asymmetry. *Science* **300**, 2040-1.

Habas, R., Dawid, I. B. and He, X. (2003). Coactivation of Rac and Rho by Wnt/Frizzled signaling is required for vertebrate gastrulation. *Genes Dev* **17**, 295-309.

Habas, R., Kato, Y. and He, X. (2001). Wnt/Frizzled activation of Rho regulates vertebrate gastrulation and requires a novel Formin homology protein Daam1. *Cell* **107**, 843-54.

Haffter, P., Granato, M., Brand, M., Mullins, M. C., Hammerschmidt, M., Kane, D. A., Odenthal, J., van Eeden, F. J., Jiang, Y. J., Heisenberg, C. P. et al. (1996). The identification of genes with unique and essential functions in the development of the zebrafish, Danio rerio. *Development* **123**, 1-36.

Hammerschmidt, M., Pelegri, F., Mullins, M. C., Kane, D. A., Brand, M., van Eeden, F. J., Furutani-Seiki, M., Granato, M., Haffter, P., Heisenberg, C. P. et al. (1996). Mutations affecting morphogenesis during gastrulation and tail formation in the zebrafish, Danio rerio. *Development* **123**, 143-51.

Heisenberg, C. P., Tada, M., Rauch, G. J., Saude, L., Concha, M. L., Geisler, R., Stemple, D. L., Smith, J. C. and Wilson, S. W. (2000). Silberblick/Wnt11 mediates convergent extension movements during zebrafish gastrulation. *Nature* **405**, 76-81.

Hwang, E., Kusch, J., Barral, Y. and Huffaker, T. C. (2003). Spindle orientation in Saccharomyces cerevisiae depends on the transport of microtubule ends along polarized actin cables. *J Cell Biol* **161**, 483-8.

Jan, Y. N. and Jan, L. Y. (2001). Asymmetric cell division in the Drosophila nervous system. *Nat Rev Neurosci* **2**, 772-9.

Jessen, J. R., Topczewski, J., Bingham, S., Sepich, D. S., Marlow, F., Chandrasekhar, A. and Solnica-Krezel, L. (2002). Zebrafish trilobite identifies new roles for Strabismus in gastrulation and neuronal movements. *Nat Cell Biol* **4**, 610-5.

Kaltschmidt, J. A., Davidson, C. M., Brown, N. H. and Brand, A. H. (2000). Rotation and asymmetry of the mitotic spindle direct asymmetric cell division in the developing central nervous system. *Nat Cell Biol* **2**, 7-12.

Keller, R. (2002). Shaping the vertebrate body plan by polarized embryonic cell movements. *Science* **298**, 1950-4.

Keller, R., Davidson, L., Edlund, A., Elul, T., Ezin, M., Shook, D. and Skoglund, P. (2000). Mechanisms of convergence and extension by cell intercalation. *Philos Trans R Soc Lond B Biol Sci* **355**, 897-922.

Keller, R., Shih, J. and Sater, A. (1992). The cellular basis of the convergence and extension of the Xenopus neural plate. *Dev Dyn* **193**, 199-217.

Keller, R. E. (1980). The cellular basis of epiboly: an SEM study of deep-cell rearrangement during gastrulation in Xenopus laevis. *J Embryol Exp Morphol* **60**, 201-34.

Kibar, Z., Vogan, K. J., Groulx, N., Justice, M. J., Underhill, D. A. and Gros, P. (2001). Ltap, a mammalian homolog of Drosophila Strabismus/Van Gogh, is altered in the mouse neural tube mutant Loop-tail. *Nat Genet* **28**, 251-5.

Kilian, B., Mansukoski, H., Barbosa, F. C., Ulrich, F., Tada, M. and Heisenberg, C. P. (2003). The role of Ppt/Wnt5 in regulating cell shape and movement during zebrafish gastrulation. *Mech Dev* **120**, 467-76.

Kim, S. H., Yamamoto, A., Bouwmeester, T., Agius, E. and Robertis, E. M. (1998). The role of paraxial protocadherin in selective adhesion and cell movements of the mesoderm during Xenopus gastrulation. *Development* **125**, 4681-90.

Kimmel, C. B., Warga, R. M. and Kane, D. A. (1994). Cell cycles and clonal strings during formation of the zebrafish central nervous system. *Development* **120**, 265-76.

Kinoshita, N., Iioka, H., Miyakoshi, A. and Ueno, N. (2003). PKC delta is essential for Dishevelled function in a noncanonical Wnt pathway that regulates Xenopus convergent extension movements. *Genes Dev* **17**, 1663-76.

Korinek, W. S., Copeland, M. J., Chaudhuri, A. and Chant, J. (2000). Molecular linkage underlying microtubule orientation toward cortical sites in yeast. *Science* **287**, 2257-9.

Kraut, R., Chia, W., Jan, L. Y., Jan, Y. N. and Knoblich, J. A. (1996). Role of inscuteable in orienting asymmetric cell divisions in Drosophila. *Nature* **383**, 50-5.

Lee, C. H. and Gumbiner, B. M. (1995). Disruption of gastrulation movements in Xenopus by a dominant-negative mutant for C-cadherin. *Dev Biol* **171**, 363-73.

Lee, L., Tirnauer, J. S., Li, J., Schuyler, S. C., Liu, J. Y. and Pellman, D. (2000). Positioning of the mitotic spindle by a cortical-microtubule capture mechanism. *Science* **287**, 2260-2.

Lee, W. L., Oberle, J. R. and Cooper, J. A. (2003). The role of the lissencephaly protein Pac1 during nuclear migration in budding yeast. *J Cell Biol* **160**, 355-64.

Liakopoulos, D., Kusch, J., Grava, S., Vogel, J. and Barral, Y. (2003). Asymmetric loading of Kar9 onto spindle poles and microtubules ensures proper spindle alignment. *Cell* **112**, 561-74.

Lu, B., Roegiers, F., Jan, L. Y. and Jan, Y. N. (2001). Adherens junctions inhibit asymmetric division in the Drosophila epithelium. *Nature* **409**, 522-5.

Lu, B., Usui, T., Uemura, T., Jan, L. and Jan, Y. N. (1999). Flamingo controls the planar polarity of sensory bristles and asymmetric division of sensory organ precursors in Drosophila. *Curr Biol* **9**, 1247-50.

Marlow, F., Topczewski, J., Sepich, D. and Solnica-Krezel, L. (2002). Zebrafish Rho kinase 2 acts downstream of Wnt11 to mediate cell polarity and effective convergence and extension movements. *Curr Biol* **12**, 876-84.

Marsden, M. and DeSimone, D. W. (2001). Regulation of cell polarity, radial intercalation and epiboly in Xenopus: novel roles for integrin and fibronectin. *Development* **128**, 3635-47.

Marsden, M. and DeSimone, D. W. (2003). Integrin-ECM interactions regulate cadherin-dependent cell adhesion and are required for convergent extension in Xenopus. *Curr Biol* **13**, 1182-91.

McNeill, H. (2002). Planar polarity: location, location, location. *Curr Biol* **12**, R449-51.

Miller, R. K., Cheng, S. C. and Rose, M. D. (2000). Bim1p/Yeb1p mediates the Kar9p-dependent cortical attachment of cytoplasmic microtubules. *Mol Biol Cell* **11**, 2949-59.

Moon, R. T., Campbell, R. M., Christian, J. L., McGrew, L. L., Shih, J. and Fraser, S. (1993). Xwnt-5A: a maternal Wnt that affects morphogenetic movements after overexpression in embryos of Xenopus laevis. *Development* **119**, 97-111.

Myers, D. C., Sepich, D. S. and Solnica-Krezel, L. (2002). Bmp activity gradient regulates convergent extension during zebrafish gastrulation. *Dev Biol* **243**, 81-98.

Nelson, W. J. (2003). Adaptation of core mechanisms to generate cell polarity. *Nature* **422**, 766-74.

Nutt, S. L., Dingwell, K. S., Holt, C. E. and Amaya, E. (2001). Xenopus Sprouty2 inhibits FGF-mediated gastrulation movements but does not affect mesoderm induction and patterning. *Genes Dev* **15**, 1152-66.

Papan, C. and Campos-Ortega, J. A. (1994). On the formation of the neural keel and neural tube in the zebrafish Danio (braquydanio) rerio. *Roux's Arch. Dev. Biol.* **203**.

Park, M. and Moon, R. T. (2002). The planar cell-polarity gene stbm regulates cell behaviour and cell fate in vertebrate embryos. *Nat Cell Biol* **4**, 20-5.

Penzo-Mendez, A., Umbhauer, M., Djiane, A., Boucaut, J. C. and Riou, J. F. (2003). Activation of Gbetagamma signaling downstream of Wnt-11/Xfz7 regulates Cdc42 activity during Xenopus gastrulation. *Dev Biol* **257**, 302-14.

Rauch, G. J., Hammerschmidt, M., Blader, P., Schauerte, H. E., Strahle, U., Ingham, P. W., McMahon, A. P. and Haffter, P. (1997). Wnt5 is required for tail formation in the zebrafish embryo. *Cold Spring Harb Symp Quant Biol* **62**, 227-34.

Roegiers, F., Younger-Shepherd, S., Jan, L. Y. and Jan, Y. N. (2001). Two types of asymmetric divisions in the Drosophila sensory organ precursor cell lineage. *Nat Cell Biol* **3**, 58-67.

Rosenblatt, J., Cramer, L. P., Baum, B. and McGee, K. M. (2004). Myosin II-dependent cortical movement is required for centrosome separation and positioning during mitotic spindle assembly. *Cell* **117**, 361-72.

Rothbacher, U., Laurent, M. N., Deardorff, M. A., Klein, P. S., Cho, K. W. and Fraser, S. E. (2000). Dishevelled phosphorylation, subcellular localization and multimerization regulate its role in early embryogenesis. *Embo J* **19**, 1010-22.

Schneider, S. Q. and Bowerman, B. (2003). Cell polarity and the cytoskeleton in the Caenorhabditis elegans zygote. *Annu Rev Genet* **37**, 221-49.

Schuyler, S. C. and Pellman, D. (2001). Search, capture and signal: games microtubules and centrosomes play. *J Cell Sci* **114**, 247-55.

Sheeman, B., Carvalho, P., Sagot, I., Geiser, J., Kho, D., Hoyt, M. A. and Pellman, D. (2003). Determinants of S. cerevisiae dynein localization and

activation: implications for the mechanism of spindle positioning. *Curr Biol* **13**, 364-72.

Shih, J. and Keller, R. (1992a). Cell motility driving mediolateral intercalation in explants of Xenopus laevis. *Development* **116**, 901-14.

Shih, J. and Keller, R. (1992b). Patterns of cell motility in the organizer and dorsal mesoderm of Xenopus laevis. *Development* **116**, 915-30.

Shimada, Y., Usui, T., Yanagawa, S., Takeichi, M. and Uemura, T. (2001). Asymmetric colocalization of Flamingo, a seven-pass transmembrane cadherin, and Dishevelled in planar cell polarization. *Curr Biol* **11**, 859-63.

Strutt, D. (2003). Frizzled signalling and cell polarisation in Drosophila and vertebrates. *Development* **130**, 4501-13.

Strutt, D., Johnson, R., Cooper, K. and Bray, S. (2002). Asymmetric localization of frizzled and the determination of notch-dependent cell fate in the Drosophila eye. *Curr Biol* **12**, 813-24.

Tada, M. and Smith, J. C. (2000). Xwnt11 is a target of Xenopus Brachyury: regulation of gastrulation movements via Dishevelled, but not through the canonical Wnt pathway. *Development* **127**, 2227-38.

Takeuchi, M., Nakabayashi, J., Sakaguchi, T., Yamamoto, T. S., Takahashi, H., Takeda, H. and Ueno, N. (2003). The prickle-related gene in vertebrates is essential for gastrulation cell movements. *Curr Biol* **13**, 674-9.

Topczewski, J., Sepich, D. S., Myers, D. C., Walker, C., Amores, A., Lele, Z., Hammerschmidt, M., Postlethwait, J. and Solnica-Krezel, L. (2001). The zebrafish glypican knypek controls cell polarity during gastrulation movements of convergent extension. *Dev Cell* **1**, 251-64.

Tree, D. R., Ma, D. and Axelrod, J. D. (2002). A three-tiered mechanism for regulation of planar cell polarity. *Semin Cell Dev Biol* **13**, 217-24.

Ulrich, F., Concha, M. L., Heid, P. J., Voss, E., Witzel, S., Roehl, H., Tada, M., Wilson, S. W., Adams, R. J., Soll, D. R. et al. (2003). Slb/Wnt11 controls hypoblast cell migration and morphogenesis at the onset of zebrafish gastrulation. *Development*.

Vaughan, P. S., Leszyk, J. D. and Vaughan, K. T. (2001). Cytoplasmic dynein intermediate chain phosphorylation regulates binding to dynactin. *J Biol Chem* **276**, 26171-9.

Veeman, M. T., Axelrod, J. D. and Moon, R. T. (2003a). A second canon. Functions and mechanisms of beta-catenin-independent Wnt signaling. *Dev Cell* **5**, 367-77.

Veeman, M. T., Slusarski, D. C., Kaykas, A., Louie, S. H. and Moon, R. T. (2003b). Zebrafish prickle, a modulator of noncanonical Wnt/Fz signaling, regulates gastrulation movements. *Curr Biol* **13**, 680-5.

Wallingford, J. B., Ewald, A. J., Harland, R. M. and Fraser, S. E. (2001). Calcium signaling during convergent extension in Xenopus. *Curr Biol* **11**, 652-61.

Wallingford, J. B., Fraser, S. E. and Harland, R. M. (2002). Convergent extension: the molecular control of polarized cell movement during embryonic development. *Dev Cell* **2**, 695-706.

Wallingford, J. B. and Harland, R. M. (2002). Neural tube closure requires Dishevelled-dependent convergent extension of the midline. *Development* **129**, 5815-25.

Wallingford, J. B., Rowning, B. A., Vogeli, K. M., Rothbacher, U., Fraser, S. E. and Harland, R. M. (2000). Dishevelled controls cell polarity during Xenopus gastrulation. *Nature* **405**, 81-5.

Warga, R. M. and Kimmel, C. B. (1990). Cell movements during epiboly and gastrulation in zebrafish. *Development* **108**, 569-80.

Wilson, P. and Keller, R. (1991). Cell rearrangement during gastrulation of Xenopus: direct observation of cultured explants. *Development* **112**, 289-300.

Winklbauer, R. and Keller, R. E. (1996). Fibronectin, mesoderm migration, and gastrulation in Xenopus. *Dev Biol* **177**, 413-26.

Winklbauer, R. and Nagel, M. (1991). Directional mesoderm cell migration in the Xenopus gastrula. *Dev Biol* **148**, 573-89.

Yamamoto, A., Amacher, S. L., Kim, S. H., Geissert, D., Kimmel, C. B. and De Robertis, E. M. (1998). Zebrafish paraxial protocadherin is a downstream target of spadetail involved in morphogenesis of gastrula mesoderm. *Development* **125**, 3389-97.

Yanagawa, S., van Leeuwen, F., Wodarz, A., Klingensmith, J. and Nusse, R. (1995). The dishevelled protein is modified by wingless signaling in Drosophila. *Genes Dev* **9**, 1087-97.

Yeo, S. Y., Little, M. H., Yamada, T., Miyashita, T., Halloran, M. C., Kuwada, J. Y., Huh, T. L. and Okamoto, H. (2001). Overexpression of a slit homologue impairs convergent extension of the mesoderm and causes cyclopia in embryonic zebrafish. *Dev Biol* **230**, 1-17.

Yin, H., Pruyne, D., Huffaker, T. C. and Bretscher, A. (2000). Myosin V orientates the mitotic spindle in yeast. *Nature* **406**, 1013-5.

Zhong, Y., Brieher, W. M. and Gumbiner, B. M. (1999). Analysis of C-cadherin regulation during tissue morphogenesis with an activating antibody. *J Cell Biol* **144**, 351-9.